

Part III

Corrosion inhibition studies

Chapter 3

Nimmy Kuriakose “Physicochemical, thermoanalytical, electrochemical and antitumour studies of transition metal complexes of schiff bases derived from heterocyclic carbonyl compounds” Thesis. Department of Chemistry, St. Thomas College, University of Calicut, 2015

CHAPTER 3

CORROSION INHIBITION INVESTIGATIONS ON SCHIFF BASE INHIBITORS I3YT2YMAPA, T2YMABA, PHMT2YBA, CTHMT2YBA AND CTHMF2YBA ON MILD STEEL IN ACIDIC MEDIA

Five different heterocyclic Schiff base inhibitors, 3-(1H-indol-3-yl)-2-[(E)-(thiophen-2-ylmethylidene)amino]propanoic acid (I3YT2YMAPA), (E)-3-[thiophen-2-ylmethylene amino]benzoic acid (T2YMABA), (E)-4-(5-[(2-phenylhydrazono)methyl]thiophen-2-yl)benzoic acid (PHMT2YBA), (E)-4-(5-[(2-carbamothioylhydrazono)methyl]thiophen-2-yl)benzoic acid (CTHMT2YBA) and (E)-4-(5-[(2-carbamothioylhydrazono)methyl]furan-2-yl)benzoic acid (CTHMF2YBA) were synthesized and characterised as described in part I. The corrosion inhibition efficiencies of these compounds on mild steel (MS) in hydrochloric acid and sulphuric acid medium were investigated using the conventional gravimetric studies and electrochemical studies like potentiodynamic polarization and electrochemical impedance spectroscopic studies. Adsorption studies were conducted to analyse the mechanism by which these Schiff bases exhibit corrosion inhibition. To determine thermodynamic parameters of corrosion, corrosion rates of mild steel in aggressive medium at different temperatures were also estimated. Surface morphological analysis was also conducted using scanning electron microscopy.

This chapter is divided into two sections; Section I describes the corrosion inhibition behaviour of the Schiff base inhibitors in 1.0M hydrochloric acid medium and Section II deals with their corrosion inhibition behaviour in 0.5M sulphuric acid medium. In each section the weight loss measurements, electrochemical impedance spectroscopic analyses and potentiodynamic polarization studies are described.

SECTION I

CORROSION INHIBITION STUDIES OF SCHIFF BASE INHIBITORS I3YT2YMAPA, T2YMABA, PHMT2YBA, CTHMT2YBA AND CTHMF2YBA ON MILD STEEL IN 1.0M HCl

The corrosion inhibition studies of the Schiff base inhibitors I3YT2YMAPA, T2YMABA, PHMT2YBA, CTHMT2YBA and CTHMF2YBA were conducted in 1.0M HCl by preparing inhibitor solutions in the range 0.2mM-1.0mM. The MS specimens used for the study were prepared in accordance with ASTM standards. Weight loss studies and electrochemical studies were performed to evaluate the inhibition capacities of these inhibitors.

Weight loss studies

The well polished MS specimens were immersed in hydrochloric acid medium in the presence and absence of the Schiff base inhibitors. The weight loss occurred for the specimens after 24 h were noted and corrosion rates were calculated. Each Schiff base inhibitor gave different corrosion inhibition values characteristic of each one.

Table 3.1 exhibits the corrosion rates of mild steel in 1.0M HCl in the presence of various concentrations of Schiff bases. The corrosion rates of steel specimens appreciably decreased in all cases with the inhibitor concentration. The metal specimen immersed in the acid solution in the absence of Schiff base showed a corrosion rate of 5.94 mm/y. On close comparison of the corrosion rates it is understandable that the mild steel specimen in HCl solution in the presence of Schiff base I3YT2YMAPA displayed appreciable lower corrosion rate. The decrease in the corrosion rate with the inhibitor concentration suggests that the metal dissolution process is considerably hindered by the azomethine

molecules. Figure 3.6 compares the corrosion rates of mild steel specimens in the presence of varying concentrations of imines.

Table 3.1 Corrosion rates of MS in $\text{mm} \cdot \text{year}^{-1}$ in the presence and absence of Schiff base inhibitors I3YT2YMAPA, T2YMABA, PHMT2YBA, CTHMT2YBA and CTHMF2YBA in 1.0M HCl

C (mM)	Inhibitors				
	I3YT2YMAPA	T2YMABA	PHMT2YBA	CTHMT2YBA	CTHMF2YBA
0	5.94	5.94	5.94	5.94	5.94
0.2	3.96	4.43	4.03	4.64	4.53
0.4	2.98	3.19	3.48	3.98	4.19
0.6	2.15	2.79	1.93	2.66	2.99
0.8	1.72	1.95	1.85	2.36	1.88
1.0	0.96	1.60	1.17	1.56	1.66

Corrosion inhibition efficiencies of Schiff bases on mild steel in HCl medium were investigated and reported in Table3.2. Figure 3.7 compares the inhibition efficiencies of Schiff bases at various concentrations on MS. It is unambiguous from the data that all azomethines showed fair corrosion inhibition efficiencies against the metallic corrosion especially the MS corrosion. The inhibition efficiencies were increased with the inhibitor concentrations. At a maximum concentration of 1.0mM, Schiff bases displayed 70-83% inhibition efficiencies. It was difficult to increase the concentration of imines in acid medium due to their poor solubility and therefore the corrosion investigations were limited in the concentration range 0.2 - 1.0mM. On examination of the data it is evident that the Schiff base I3YT2YMAPA showed pronounced corrosion inhibition efficiency than all other Schiff bases at all concentrations. The enhanced efficiency of this molecule

can be correlated with its molecular structure. Presence of two aromatic ring system; one from the aldehyde part and other from amino part together with azomethine linkage and nitrogen atom of the indole moiety make the molecule so electron rich which help to bind on the surface metal atoms of mild steel. In addition to this, the molecules possess almost planar structure which was confirmed by the optimized geometry determination and this scenario is beneficial to the strong binding of the molecule on the metal surface.

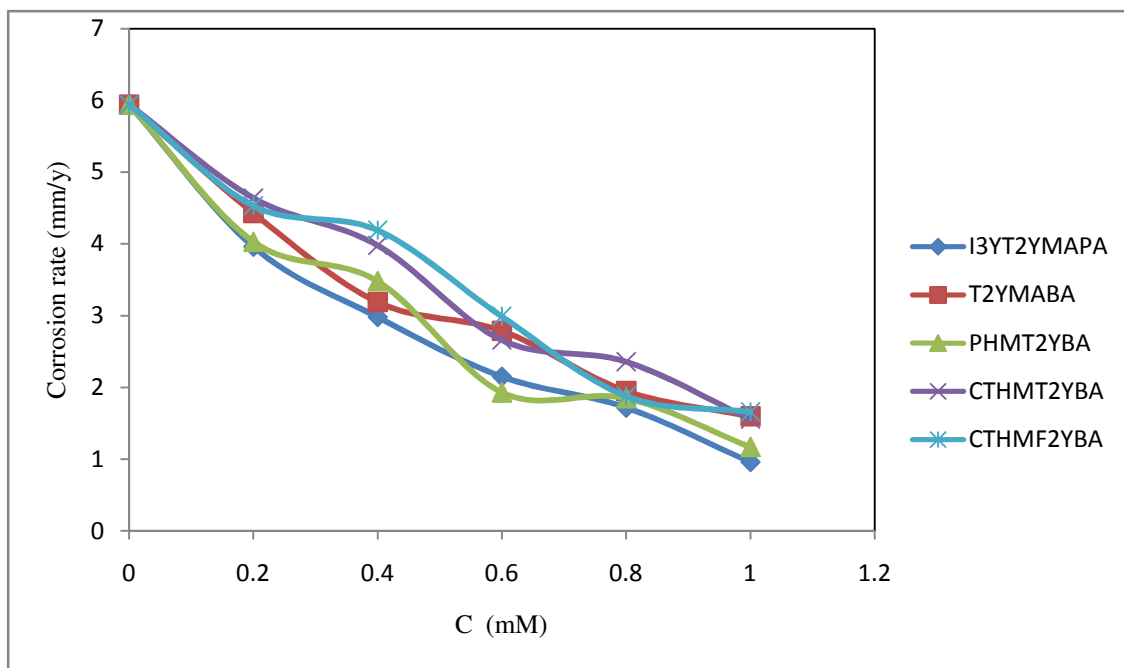


Fig. 3.6 Variation of corrosion rates of MS with the concentration of Schiff base inhibitors I3YT2YMAPA, T2YMABA, PHMT2YBA, CTHMT2YBA and CTHMF2YBA in 1.0M HCl

The Schiff base PHMT2YBA also showed appreciable inhibition efficiency against mild steel corrosion. A maximum of 80% inhibition efficiency was achieved by this molecule at a concentration of 1.0mM. This molecule possess three aromatic ring systems; two from the aldehyde side and one from amino part. The electron density of the aromatic ring systems, azomethine linkage and highly polarisable sulphur atom are the root causes in which the molecule showed better inhibition efficiency. Even though the

molecule is not planar completely as per the optimized geometry, the two benzene rings and the sulphur atom remain in the same plane, which is a fair condition to adsorb the molecule on the metal surface.

Table 3.2 Inhibition efficiencies of Schiff base inhibitors I3YT2YMAPA, T2YMABA, PHMT2YBA, CTHMT2YBA and CTHMF2YBA on MS in 1.0M HCl

C (mM)	Inhibitors				
	I3YT2YMAPA	T2YMABA	PHMT2YBA	CTHMT2YBA	CTHMF2YBA
0.2	33.26	25.32	32.06	20.54	23.64
0.4	49.82	46.08	41.33	32.71	29.46
0.6	63.75	52.90	67.46	55.17	49.69
0.8	71.08	67.17	68.81	60.19	69.28
1.0	83.86	72.99	80.32	73.75	71.99

The low corrosion inhibition of the molecule T2YMABA, compared to the previously described molecules, may be attributed to deviation from co-planarity in its molecular geometry. Even though the molecule is equipped with active corrosion inhibition probes, the puckered shape of the molecule prevents the appreciable interaction with the metal atoms. The molecules CTHMT2YBA and CTHMF2YBA showed comparatively low corrosion inhibition efficiency. A maximum of approx. 70% efficiency was noticed by these molecules at 1.0mM concentration. On comparing the structures of two molecules, one can understand that the only difference between the two molecules is presence of sulphur in former which is replaced by oxygen atom in the second one. Even though the first molecule is equipped with more electron rich sulphur atom, the molecule is somewhat more puckered than the other one. The second one contains more electron negative oxygen as the hetero atom, but achieved more planar

structures. These two molecules displayed almost same corrosion inhibition efficiencies on mild steel surface. Figure 3.8 shows the optimized geometries of the Schiff base inhibitors.

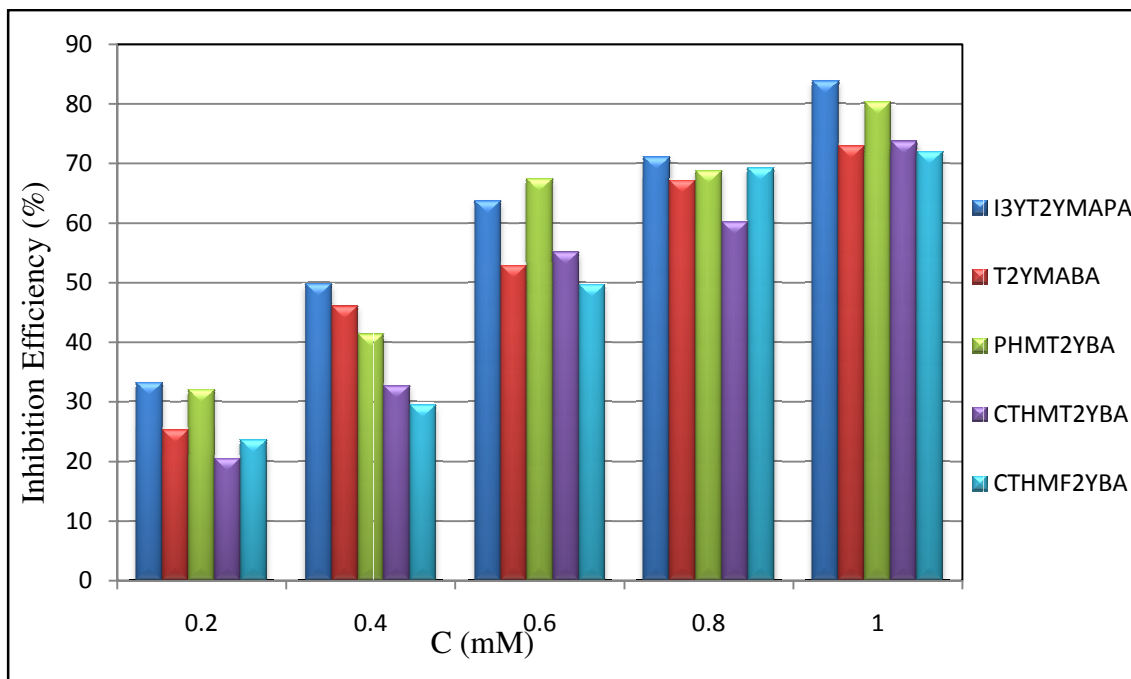
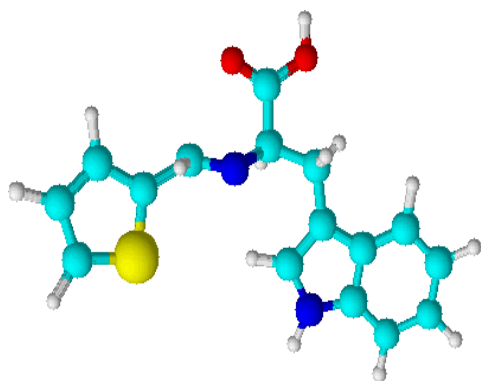
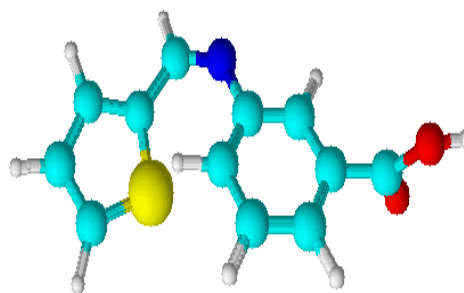


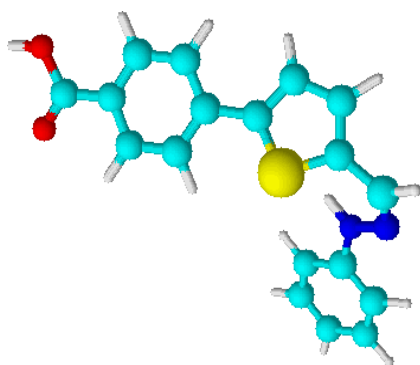
Fig. 3.7 Comparison of corrosion inhibition efficiencies ($\eta_w\%$) of Schiff base inhibitors I3YT2YMAPA, T2YMABA, PHMT2YBA, CTHMT2YBA and CTHMF2YBA on MS in 1.0M HCl



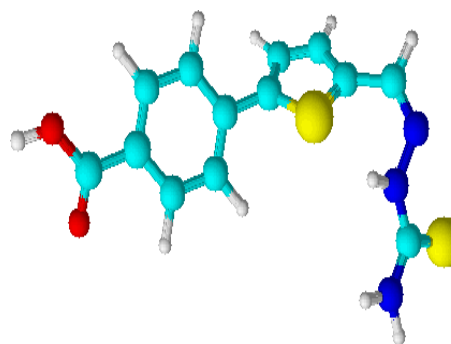
3-(1H-indol-3-yl)-2-[(E)-(thiophen-2-ylmethylidene)amino]propanoic acid (I3YT2YMAPA)



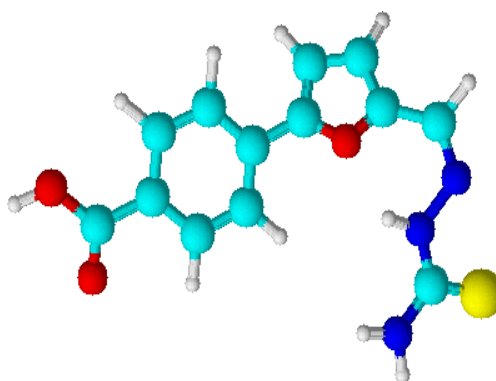
(E)-3-[thiophen-2-ylmethyleneamino] benzoic acid (T2YMABA)



(E)-4-(5-[(2-phenylhydrazono)methyl]thiophen-2-yl) benzoic acid (PHMT2YBA)



(E)-4-(5-[(2-carbamothioylhydrazono)methyl]thiophen-2-yl)benzoic acid (CTHMT2YBA)



(E)-4-(5-[(2-carbamothioylhydrazono)methyl]furan-2-yl)benzoic acid (CTHMF2YBA)

Fig. 3.8 Optimized geometries of Schiff base molecules

Comparison of corrosion inhibition efficiencies of Schiff base inhibitors with their parent amines

The corrosion inhibition behaviour of Schiff base inhibitors were compared with their parent amines at three different concentrations. The results are given in Table 3.3. The parent amines such as 2-amino-3-(3-indolyl)propionic acid (AIPA), 3-aminobenzoic acid (3ABA), thiocarbamoyl hydrazide (TCH) and phenyl hydrazine (PH) exhibited much lower corrosion inhibition on MS when compared to that of the Schiff bases. The superior inhibitory power of the Schiff base inhibitors was clearly established, which can be attributed to the presence of azomethine linkage. The results are pictured in Figure 3.9.

Table 3.3 Corrosion inhibition efficiencies ($\eta_w\%$) of Schiff base inhibitors I3YT2YMAPA, T2YMABA, PHMT2YBA, CTHMT2YBA, CTHMF2YBA and their parent amines in 1.0M HCl

Compounds	Concentration (mM)		
	0.2	0.6	1.0
AIPA	10.27	31.18	48.42
3ABA	4.29	29.13	38.42
PH	11.91	31.85	44.33
TCH	2.49	29.54	49.86
I3YT2YMAPA	33.26	63.75	83.86
T2YMABA	25.32	52.90	72.99
PHMT2YBA	32.06	67.46	80.32
CTHMT2YBA	20.54	55.17	73.75
CTHMF2YBA	23.64	49.69	71.99

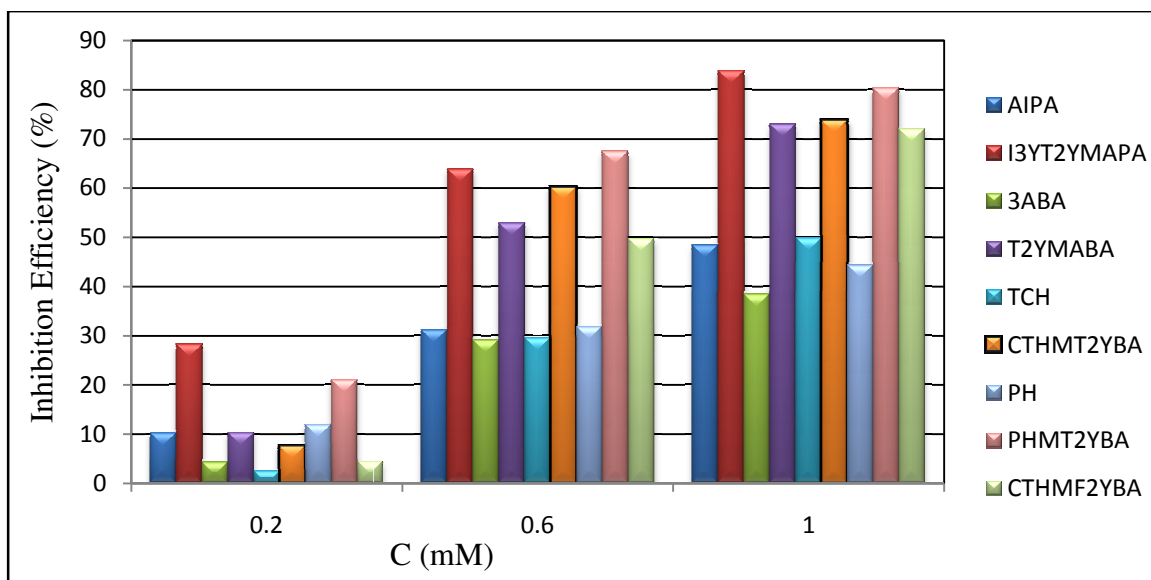


Fig. 3.9 Comparison of corrosion inhibition efficiencies ($\eta_w\%$) of Schiff base inhibitors I3YT2YMAPA, T2YMABA, PHMT2YBA, CTHMT2YBA, CTHMF2YBA and their parent amines in 1.0M HCl

Adsorption isotherms

The corrosion inhibition property of inhibitor molecules is due to the adsorption on the surface of metal specimens. The mechanism of adsorption and the surface behaviour of organic molecules can be studied by adsorption isotherms. Different models of adsorption isotherms considered are Langmuir, Temkin, Frumkin and Freundlich isotherms. For verifying the mechanism of inhibition, various adsorption isotherms were plotted and the most appropriate one with the highest correlation coefficient (R^2) was selected. Parameters like adsorption equilibrium constant K_{ads} and free energy of adsorption ΔG_{ads} were calculated from the adsorption isotherms. From the adsorption studies it was found that Schiff bases I3YT2YMAPA, PHMT2YBA, CTHMT2YBA and CTHMF2YBA followed Freundlich adsorption isotherm during the inhibition process on the MS surface. Langmuir isotherm was obeyed by T2YMABA

molecules. The adsorption isotherms are represented in the Figures 3.10 to 3.14 and the parameters obtained by the analysis of isotherms are listed in Table 3.4.

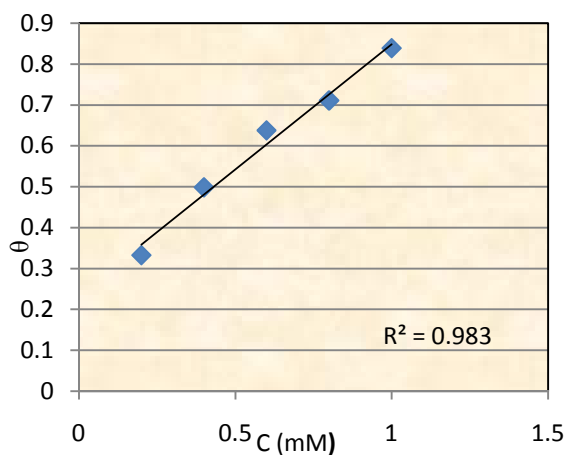


Fig. 3.10 Freundlich adsorption isotherm for I3YT2YMAPA on MS in 1.0M HCl

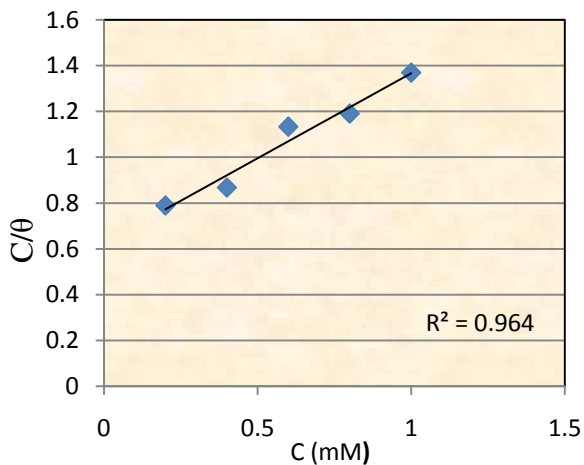


Fig. 3.11 Langmuir adsorption isotherm for T2YMABA on MS in 1.0M HCl

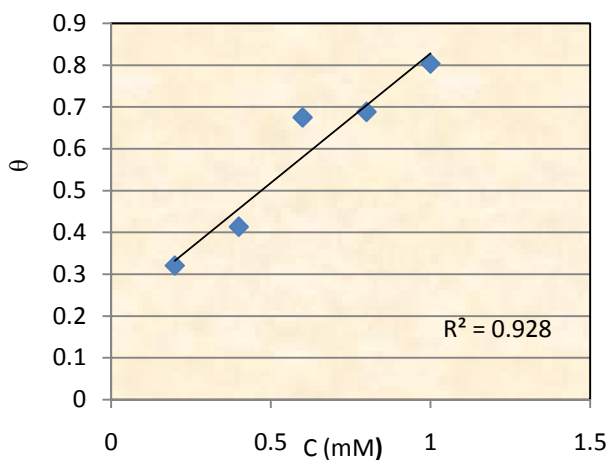


Fig. 3.12 Freundlich adsorption isotherm for PHMT2YBA on MS in 1.0M HCl

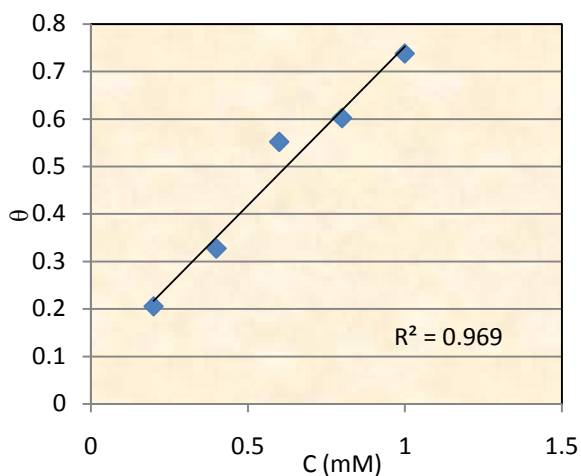


Fig. 3.13 Freundlich adsorption isotherm for CTHMT2YBA on MS in 1.0M HCl

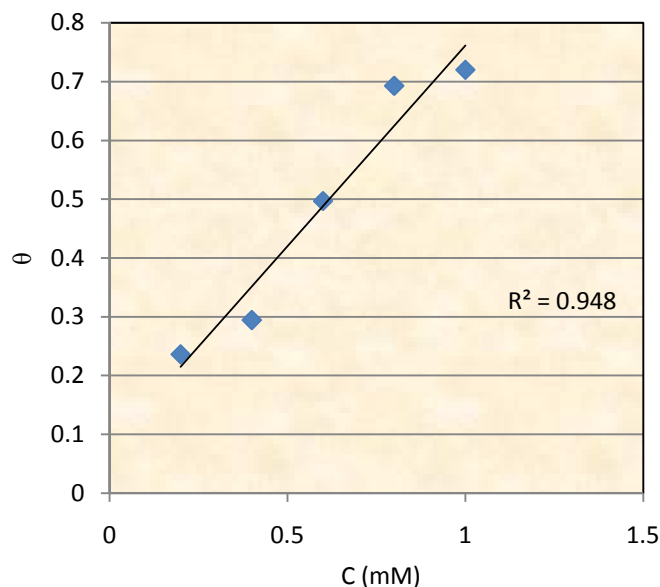


Fig. 3.14 Freundlich adsorption isotherm for CTHMF2YBA on MS in 1.0M HCl

Table 3.4 Thermodynamic parameters for the adsorption of I3YT2YMAPA, T2YMABA, PHMT2YBA, CTHMT2YBA and CTHMF2YBA on MS in 1.0M HCl

Parameter	Inhibitor				
	I3YT2YMAPA	T2YMABA	PHMT2YBA	CTHMT2YBA	CTHMF2YBA
K_{ads}	4237.29	1600	4807.69	12048.19	12820.51
ΔG_{ads}^0 (kJmol ⁻¹)	-31.18	-28.724	-31.49	-33.81	-33.96

Negative values ΔG_{ads}^0 for all Schiff base inhibitors indicate the spontaneity of the adsorption process on the metal surface. ΔG_{ads}^0 values up to -20kJ mol^{-1} indicate electrostatic interaction between the charged molecule and the charged surface of the metal through physisorption while ΔG_{ads}^0 more negative than -40kJ indicates strong adsorption of the inhibitor molecules on the metal surface through co-ordinate type bond, which is called chemisorption⁶⁷. In the case of inhibitors considered here ΔG_{ads}^0 ranges

between -28 kJmol^{-1} and -34 kJmol^{-1} for MS specimens suggesting that the adsorption of all these molecules involves both electrostatic adsorption and chemisorption. For the Schiff base inhibitors CTHMT2YBA and CTHMF2YBA, the free energy of adsorptions were comparatively higher than that of the other imines suggesting that these inhibitors are more strongly adsorbed forming a monolayer on the surface of the MS specimens through chemical interaction.

Effect of temperature

To evaluate the effect of temperature on corrosion rate of the MS specimens, weight loss studies of the Schiff base inhibitors were conducted in the temperature range $30\text{-}60^{\circ}\text{C}$. The activation energy of corrosion with and without the inhibitor was calculated by Arrhenius equation

$$K = A \exp \left(-\frac{E_a}{RT} \right) \quad (8)$$

where K is the rate of corrosion, E_a the activation energy, A the frequency factor, T the temperature in Kelvin scale and R is the gas constant. The linear plots between $\log K$ and $1000/T$ having regression coefficients close to unity indicate that the corrosion of MS in HCl can be explained by the simple kinetic model for all the Schiff bases. Plots of $\log K$ Vs $1000/T$ and $\log (K/T)$ Vs $1000/T$ in the presence and absence of the inhibitor are represented in Figures 3.15-3.24. Enthalpy and entropy of activation (ΔH^* , ΔS^*) were calculated from the transition state theory using the equation

$$K = \left(\frac{RT}{Nh} \right) \exp \left(\frac{\Delta S^*}{R} \right) \exp \left(\frac{-\Delta H^*}{RT} \right) \quad (9)$$

where N is the Avogadro number and h is the Plancks constant. Table 3.5 shows the activation energy and thermodynamic parameters of corrosion. The increase of activation energy of dissolution of the metal with increase in the inhibitor concentration implies the increase in the reluctance of dissolution of metal. Positive signs of enthalpies with a regular rise reflect the endothermic nature of dissolution and the increasing difficulty of corrosion with the inhibitor. The entropy of activation also increases with the inhibitor concentration. For the lower concentrations of the inhibitor, the entropy of activation is negative indicating that the activated molecules are in highly ordered state than that at the initial state. But as the concentration of inhibitor rises, the disordering of activated complex becomes more significant and the entropy of activation becomes positive.

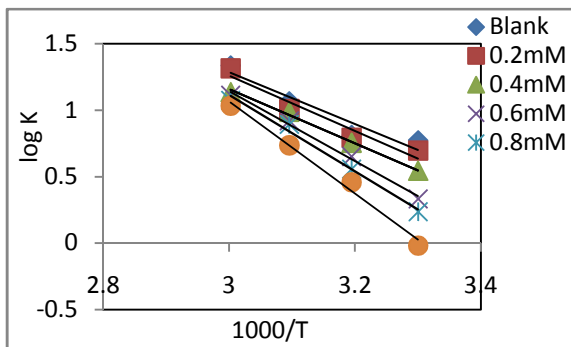


Fig. 3.15 Arrhenius plots for the corrosion of MS in the absence and presence of I3YT2YMAPA in 1.0M HCl

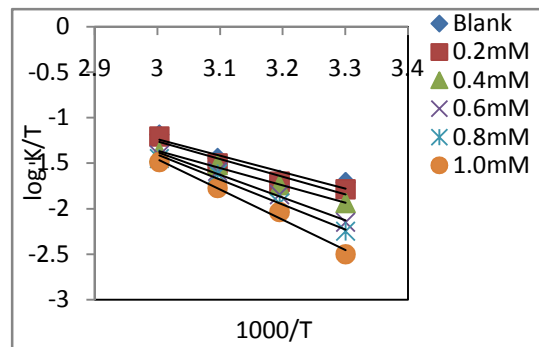


Fig. 3.16 Plots of $\log(K/T)$ vs $1000/T$ for the corrosion of MS in the absence and presence of I3YT2YMAPA in 1.0M HCl

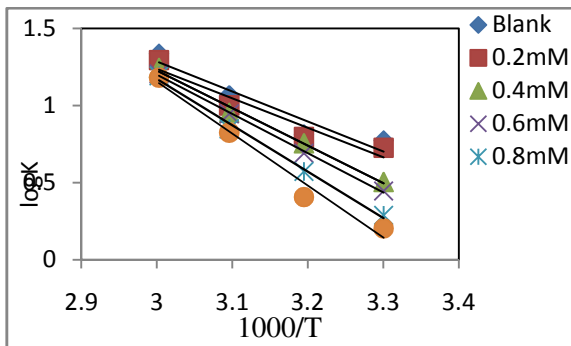


Fig. 3.17 Arrhenius plots for the corrosion of MS in the absence and presence of T2YMABA in 1.0M HCl

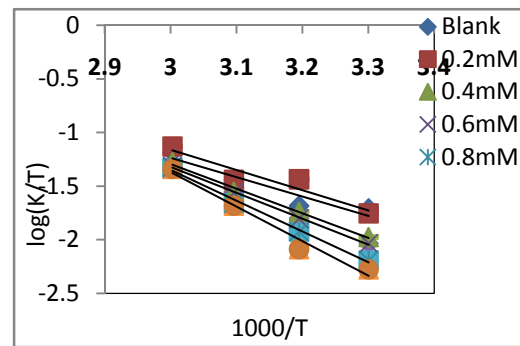


Fig. 3.18 Plots of $\log(K/T)$ vs $1000/T$ for the corrosion of MS in the absence and presence of T2YMABA in 1.0M HCl

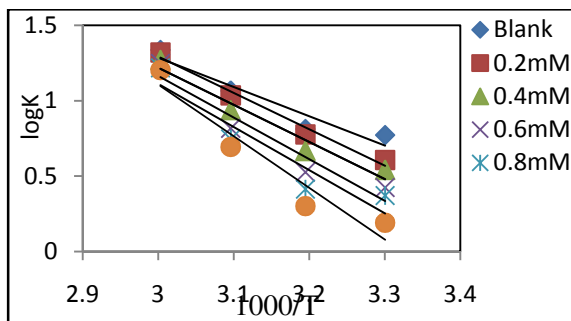


Fig. 3.19 Arrhenius plots for the corrosion of MS in the absence and presence of PHMT2YBA in 1.0M HCl

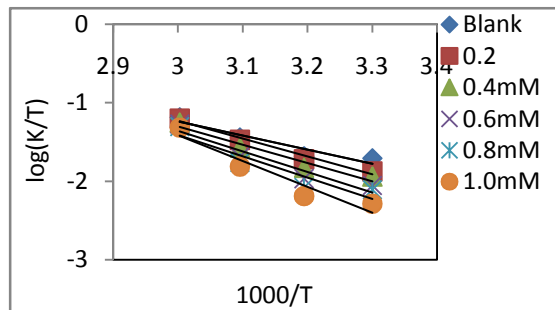


Fig. 3.20 Plots of $\log(K/T)$ vs $1000/T$ for the corrosion of MS in the absence and presence of PHMT2YBA in 1.0M HCl

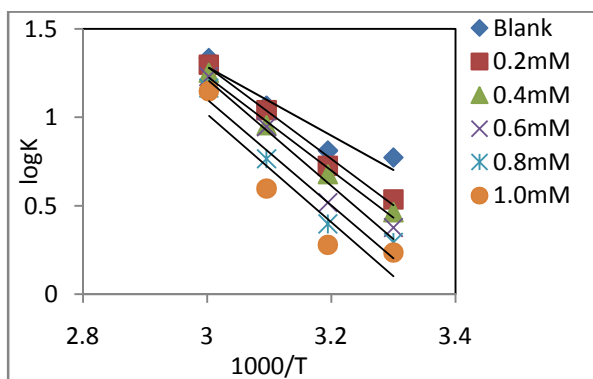


Fig. 3.21 Arrhenius plots for the corrosion of MS in the absence and presence of CTHMT2YBA in 1.0M HCl

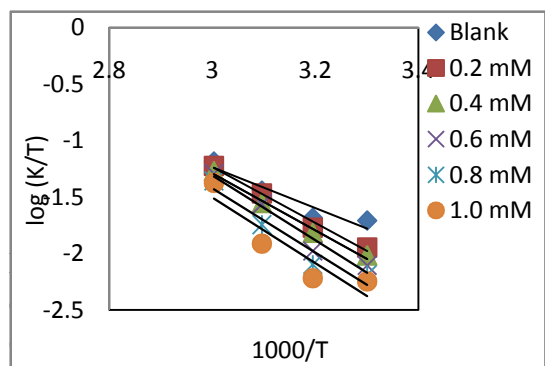


Fig. 3.22 Plots of $\log(K/T)$ vs $1000/T$ for the corrosion of MS in the absence and presence of CTHMT2YBA in 1.0M HCl

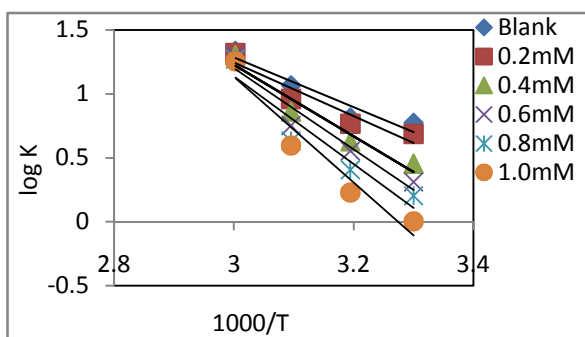


Fig. 3.23 Arrhenius plots for the corrosion of MS in the absence and presence of CTHMF2YBA in 1.0M HCl

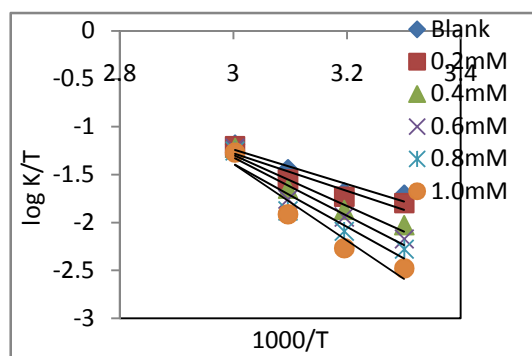


Fig. 3.24 Plots of $\log(K/T)$ vs $1000/T$ for the corrosion of MS in the absence and presence of CTHMF2YBA in 1.0M HCl

Table 3.5 Thermodynamic parameters of corrosion of MS in the presence and absence of Schiff base inhibitors I3YT2YMAPA, T2YMABA, PHMT2YBA, CTHMT2YBA, and CTHMF2YBA in 1.0M HCl

Inhibitor	C (mM)	E _a (kJ mol ⁻¹)	A	ΔH* (kJ mol ⁻¹)	ΔS* (J mol ⁻¹ K ⁻¹)
I3YT2YMAPA	Blank	37.2	1.3x10 ⁷	37.2	-61.33
	0.2	39.83	3.1X10 ⁷	39.82	-53.92
	0.4	38.96	1.8X10 ⁷	38.96	-58.51
	0.6	50.47	1.13X10 ⁹	50.5	-24.24
	0.8	55.13	5.68X10 ⁹	55.12	-10.82
	1.0	66.37	2.88X10 ¹¹	66.36	21.85
T2YMABA	0.2	36.56	9.2X10 ⁷	36.6	-64.22
	0.4	46.64	3.4X10 ⁸	46.6	-34.16
	0.6	48.83	7.1X10 ⁸	48.8	-28.09
	0.8	57.57	1.5X10 ¹⁰	57.6	-2.47
	1.0	64.39	1.72x10 ¹¹	64.4	17.64
PHMT2YBA	0.2	46.07	3.231X10 ⁸	47.1	-34.65
	0.4	47.11	3.98X10 ⁸	52.86	-32.91
	0.6	52.87	2.81X10 ⁹	54.76	-16.67
	0.8	54.76	4.92X10 ⁹	65.57	-12.003
	1.0	65.59	2.4X10 ¹¹	68.54	20.32
CTHMT2YBA	0.2	50.04	1.34X10 ⁹	50.03	-22.80
	0.4	50.91	1.61X10 ⁹	50.89	-21.27
	0.6	57.49	1.66X10 ¹⁰	57.47	-1.89
	0.8	57.22	1.15X10 ¹⁰	57.21	-4.96
	1.0	58.34	1.41X10 ¹⁰	58.32	-3.23
CTHMF2YBA	0.2	40.1	3.36X10 ⁷	40.09	-53.46
	0.4	53.41	3.93X10 ⁹	53.4	-13.88
	0.6	60.75	5.25X10 ¹⁰	60.75	7.68
	0.8	65.65	2.63X10 ¹¹	65.64	21.08
	1.0	79.07	3.31X10 ¹³	79.06	61.29

Surface morphological studies

SEM images of mild steel specimens were taken to ascertain the mechanism of action of Schiff base inhibitors on the metal surface. Figures 3.25 to 3.27 respectively show the SEM images of bare MS surface, MS specimen in 1.0M HCl and MS specimen in 1.0M HCl containing I3YT2YMAPA with 1.0mM concentration. The irregularities on the bare metal surface are due to the effect of surface polishing. In the acidic solution the metal specimens undergo severe corrosion which is evident from Figure 3.26. Comparing the textures of images 3.26 and 3.27, it can be well understood that the metal surface is less damaged in the presence of inhibitor I3YT2YMAPA, which is due to the formation of a protective film through adsorption on metal surface and thereby suppressing the rate of corrosion.

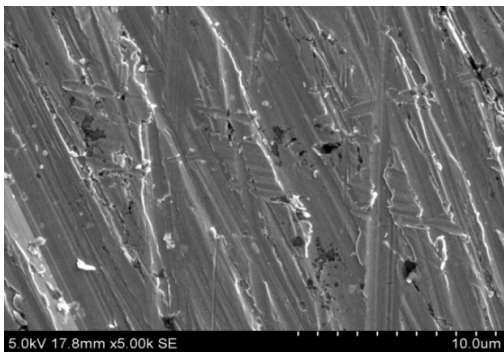


Fig. 3.25 SEM image of bare MS surface

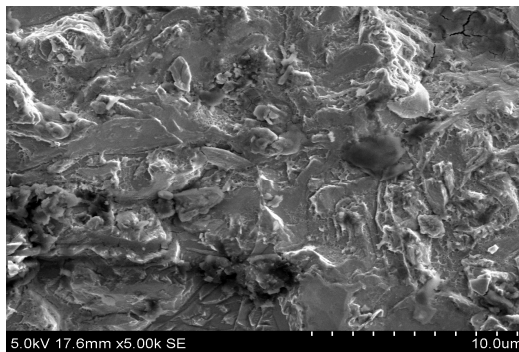


Fig. 3.26 SEM image of MS surface in 1.0M HCl (blank)



Fig. 3.27 SEM image of MS surface in 1.0M HCl and I3YT2YMAPA(1.0mM)

Electrochemical studies on corrosion

Electrochemical corrosion techniques involve EIS measurements and potentiodynamic polarization studies. These analytical methods give fast and reproducible results. The experiments were performed on three electrode assembly, in which a platinum electrode acted as the inert electrode and SCE as the reference electrode. The working electrode was 1cm² exposed area of the metal specimen. Tafel polarization measurements give data from which the prediction of the site of adsorption, whether cathodic, anodic or both. The metal specimens were immersed in the acid solution for 30 minutes prior to the analysis with and without inhibitor and the results can provide a mechanistic way to explain the inhibitive action of the various organic compounds in acidic media.

Electrochemical impedance spectroscopic studies

The impedance parameters like charge transfer resistance (R_{ct}), solution resistance (R_s), double layer capacitance (C_{dl}) and percentage inhibition efficiency ($\eta_{EIS}\%$) calculated from the R_{ct} values are given in the Table 3.6. Nyquist plots and the combined Bode-impedance plots of the five Schiff base inhibitors I3YT2YMAPA, T2YMABA, PHMT2YBA, CTHMT2YBA and CTHMF2YBA are given in Figures 3.28-3.32. The value of R_{ct} is a measure of electron transfer across the exposed area of the metal surface and it is inversely proportional to rate of corrosion. The charge transfer resistance was found to increase with the inhibitor concentration in the case of all the inhibitors. The rate of charge transfer between the metal and the solution determined the rate of metal dissolution process. The adsorbed molecules hinder the charge transfer on the metal surface. The decrease in capacitance values C_{dl} with inhibitor concentration is due to the

decrease in local dielectric constant and/or increase in the thickness of the electrical double layer⁶⁸⁻⁷⁰.

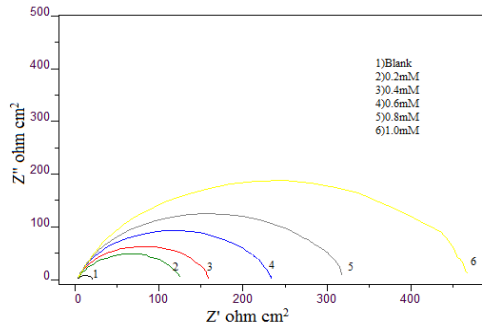


Fig3.28a Nyquist plots of MS in the presence and absence of I3YT2YMAPA in 1.0M HCl

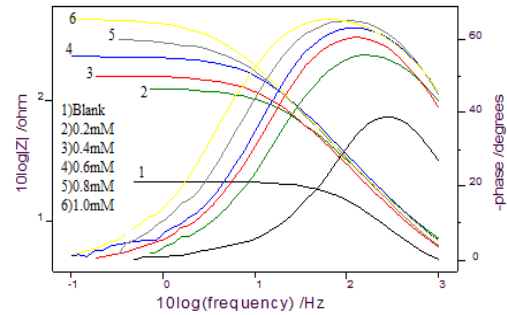


Fig. 3.28b Bode plots of MS in the presence and absence of I3YT2YMAPA in 1.0M HCl

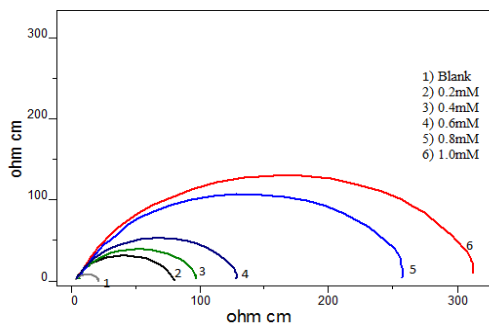


Fig. 3.29a Nyquist plots of MS in the presence and absence of T2C3ABA in 1.0M HCl

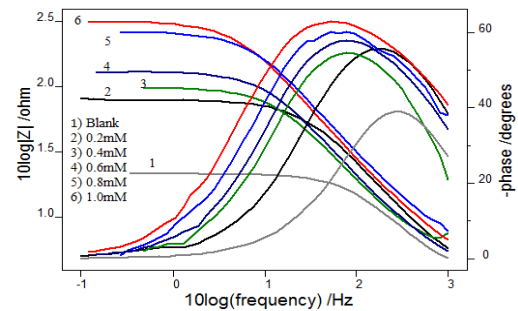


Fig. 3.29b Bode plots of MS in the presence and absence of T2C3ABA in 1.0M HCl

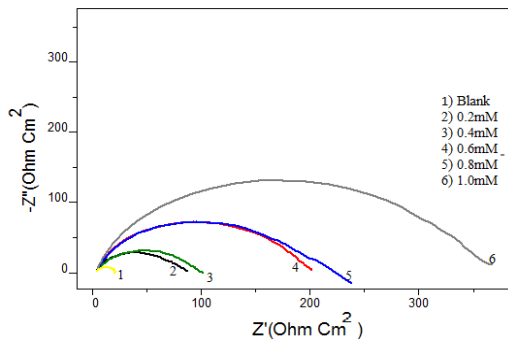


Fig. 3.30a Nyquist plots of MS in the presence and absence of PHMT2YBA in 1.0M HCl

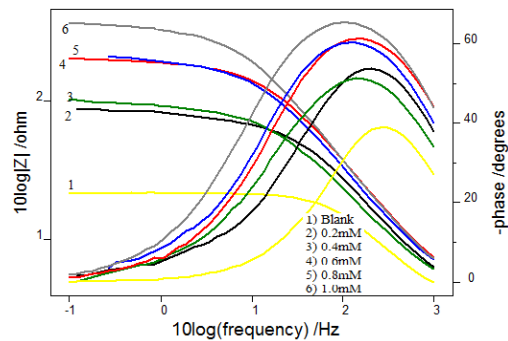


Fig. 3.30b Bode plots of MS in the presence and absence of PHMT2YBA in 1.0M HCl

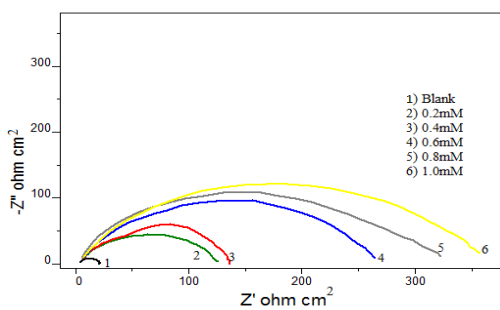


Fig. 3.31a Nyquist plots of MS in the presence and absence of CTHMT2YBA in 1.0M HCl

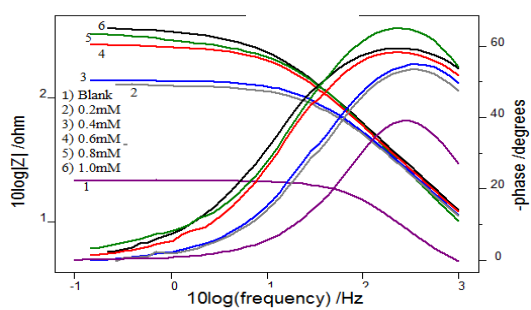


Fig. 3.31b Bode plots of MS in the presence and absence of CTHMT2YBA in 1.0M HCl

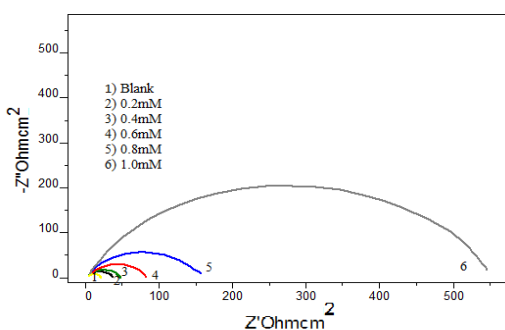


Fig. 3.32a Nyquist plots of MS in the presence and absence of CTHMF2YBA in 1.0M HCl

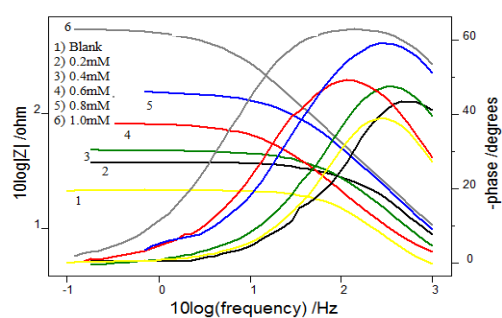


Fig. 3.32b Bode plots of MS in the presence and absence of CTHMF2YBA in 1.0M HCl

Table 3.6 Electrochemical impedance parameters of MS in the presence and absence of Schiff base inhibitors I3YT2YMAPA, T2YMABA, PHMT2YBA, CTHMT2YBA and CTHMF2YBA in 1.0M HCl

Inhibitors	C (mM)	C_{dl} ($\mu\text{F cm}^{-2}$)	R_{ct} ($\Omega \text{ cm}^{-2}$)	$\eta_{EIS}\%$
	0	95.8	16.4	-
I3YT2YMAPA	0.2	68.3	109	84.95
	0.4	77.0	142	88.45
	0.6	64.6	211	92.23
	0.8	75.5	286	94.27
	1.0	82.3	427	96.16
T2YMABA	0.2	73.4	70.3	76.67
	0.4	120	86.7	81.08
	0.6	111	117	85.99
	0.8	77.5	238	93.11
	1.0	91.7	290	94.34
PHMT2YBA	0.2	79	68.9	76.19
	0.4	113	79.6	79.39
	0.6	63.7	174	90.57
	0.8	75.6	176	90.68
	1.0	69.6	317	94.83
CTHMT2YBA	0.2	46.8	36.7	55.31
	0.4	37.0	117	85.98
	0.6	40.7	229	92.84
	0.8	41.8	269	93.90
	1.0	44.8	309	94.69
CTHMF2YBA	0.2	38.1	29	43.45
	0.4	55.5	38.8	57.73
	0.6	11.5	68.6	76.09
	0.8	38.9	131	87.48
	1.0	5.1	208	92.12

It is quite evident from the impedance data that the Schiff base inhibitor I3YT2YMAPA exhibited marked inhibition efficiency compared to others. A maximum of 96.16% was obtained with 1.0mM concentration of the inhibitor. Even at the lowest concentration, this molecule exhibited 84.95% inhibition efficiency. The presence of aromatic rings in the thiophene-2-carbaldehyde part and in the tryptophan part which involves an indole moiety made this ligand an excellent inhibitor. Besides aromatic rings, azomethine linkage also helps the molecule to bind strongly on the metal surface and to exhibit very high inhibition efficiency. The results were in good agreement with that obtained from weight loss measurements for I3YT2YMAPA.

Other inhibitors T2YMABA, PHMT2YBA, CTHMT2YBA and CTHMF2YBA also were able to produce good inhibition efficiencies even though slightly less than that of I3YT2YMAPA. The first three ligands were having almost comparable inhibition efficiency at their highest concentration, ie; around 94%. The presence of highly polarizing sulphur atom in the thiophene ring system and the azomethine linkage are responsible for their higher activities. The corrosion inhibition efficiencies of various Schiff base inhibitors are compared in Figure3.33.

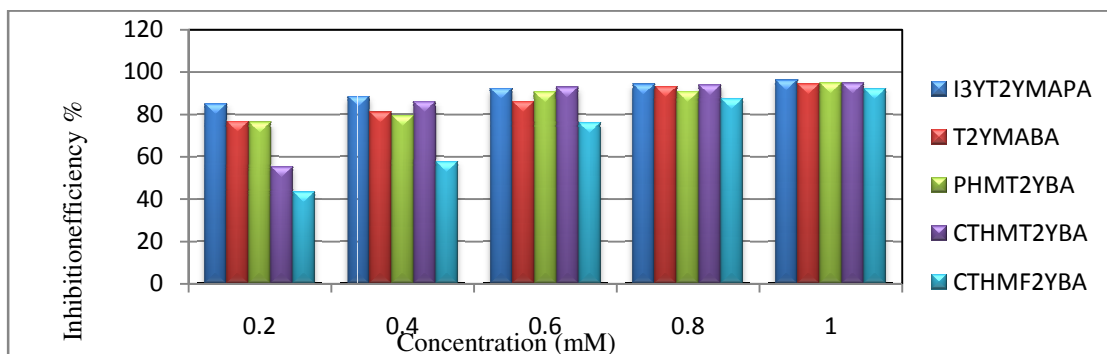


Fig. 3.33 Comparison of corrosion inhibition efficiencies ($\eta_{EIS}\%$) of Schiff bases, I3YT2YMAPA, T2YMABA, PHMT2YBA, CTHMT2YBA and CTHMF2YBA on MS in 1.0M HCl

Potentiodynamic polarization studies

The corrosion inhibition efficiencies of Schiff bases were determined by polarization studies which involve Tafel extrapolation analysis and linear polarization studies. From these techniques, corrosion parameters such as corrosion potential (E_{corr}), corrosion current density (i_{corr}), polarization resistance (R_p) were measured. Using these parameters inhibition efficiencies were determined. Figures 3.34 to 3.38 represent the Tafel plots and polarization curves of MS in the presence and absence of five Schiff base inhibitors.

Table 3.7 provides the Tafel data and linear polarization data obtained by the potentiodynamic polarization studies of all these inhibitors. In this measurement also the inhibitor I3YT2YMAPA exhibited highest inhibition efficiency in the lowest concentration compared to that of other inhibitors. The percentage of inhibition efficiencies calculated from polarisation measurements are higher than that obtained from the gravimetric studies since the analyses were carried out electrochemically and the contact time between the working electrode and the acid solution is only about half an hour whereas in the latter the contact time is 24 hours.

On analysing the data it is obvious that the corrosion current densities decreased significantly as the concentration of the Schiff bases increased. The adsorption of these organic molecules on metal surface could hinder the metal dissolution appreciably by inhibiting the anodic or cathodic process of corrosion or both. On evaluation of the Tafel and polarization curves, one can see that slope of the Tafel lines in presence of inhibitor varied considerably compared to the Tafel lines of uninhibited solution. The inhibitor can be regarded as mixed type inhibitors since the slopes of both Tafel lines are affected

considerably. If the anodic or cathodic slopes vary from the slope of the uninhibited solution, the inhibitor can be treated as an anodic or cathodic type inhibitor⁷¹.

Table 3.7 Potentiodynamic polarization parameters of MS in the presence and absence of Schiff base inhibitors, I3YT2YMAPA, T2YMABA, PHMT2YBA, CTHMT2YBA and CTHMF2YBA in 1.0M HCl

Inhibitor	Tafel Data					Linear polarization data		
	C (mM)	-E _{corr} (mV/SCE)	I _{corr} (μA/cm ²)	-b _c (mV/dec)	b _a (mV/dec)	η _{pol} %	R _p (ohm)	η _{Rp} %
I3YT2YMAPA	0	465	726	106	72	-	38.14	-
	0.2	465	141	97	79	80.58	188.9	80.79
	0.4	479	94.6	83	87	86.97	377.0	88.76
	0.6	476	53.6	85	78	92.62	463.8	92.16
	0.8	485	42.4	83	72	94.16	567.1	93.04
	1.0	476	34.1	87	89	95.33	651.2	95.25
T2YMABA	0.2	476	183	89	79	74.79	82.3	73.51
	0.4	483	174	93	89	76.03	114	80.88
	0.6	475	111	90	68	84.71	152	85.66
	0.8	479	49.2	89	79	93.22	313	93.04
	1.0	487	40.4	86	76	94.44	367.3	94.07
PHMT2YBA	0.2	501	173	83	74	76.17	86.5	74.79
	0.4	500	131	81	91	81.96	125.4	82.62
	0.6	517	76	84	100	89.53	214	89.81
	0.8	515	68	76	94	90.63	221	90.14
	1.0	516	39	85	95	94.63	405	94.62
CTHMT2YBA	0.2	510	316	103	63	56.47	47.59	54.19
	0.4	512	204	105	72	71.90	68.78	68.30
	0.6	502	132.6	99	58	81.74	173	87.39
	0.8	513	89.1	90	70	87.73	294	92.58
	1.0	499	42.2	94	51	94.19	369	94.09
CTHMF2YBA	0.2	499	222	101	63	69.43	64.33	66.11
	0.4	488	199	104	63	72.59	76.03	71.33
	0.6	497	202	109	74	72.18	78.07	72.08
	0.8	508	64	89	94	91.18	238.4	90.85
	1.0	505	56.7	83	85	92.19	305.4	92.86

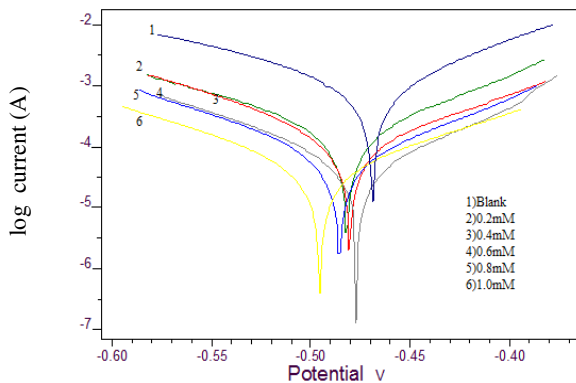


Fig. 3.34a Tafel plots of MS in the presence and absence of I3YT2YMAPA in 1.0M HCl

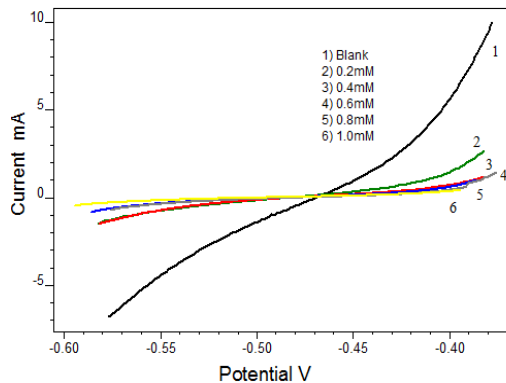


Fig. 3.34b Linear polarization curves of MS in the presence and absence of I3YT2YMAPA in 1.0M HCl

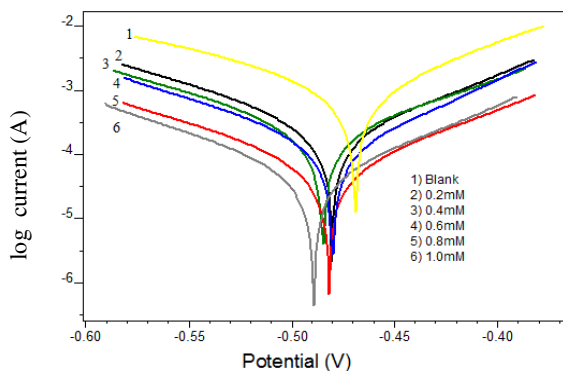


Fig. 3.35a Tafel plots of MS in the presence and absence of T2YMABA in 1.0M HCl

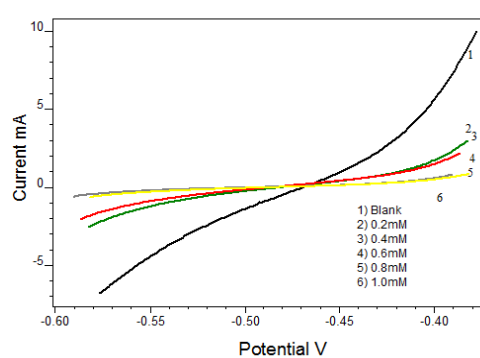


Fig. 3.35b Linear polarization curves of MS in the presence and absence of T2YMABA in 1.0M HCl

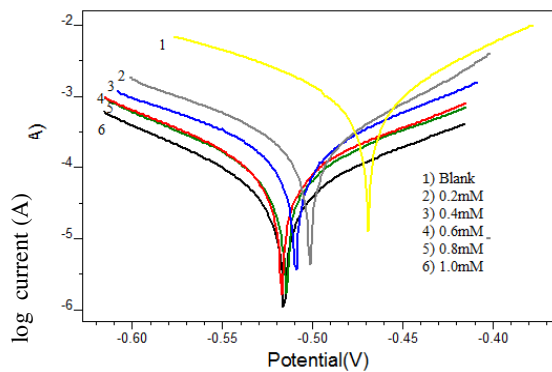


Fig. 3.36a Tafel plots of MS in the presence and absence of PHMT2YBA in 1.0M HCl

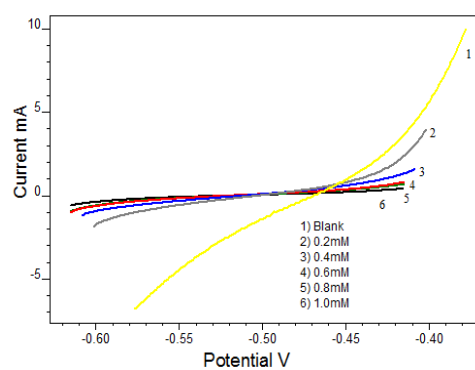


Fig. 3.36b Linear polarization curves of MS in the presence and absence of PHMT2YBA in 1.0M HCl

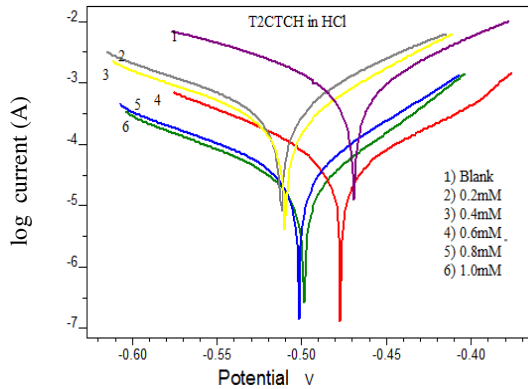


Fig. 3.37a Tafel plots of MS in the presence and absence of CTHMT2YBA in 1.0M HCl

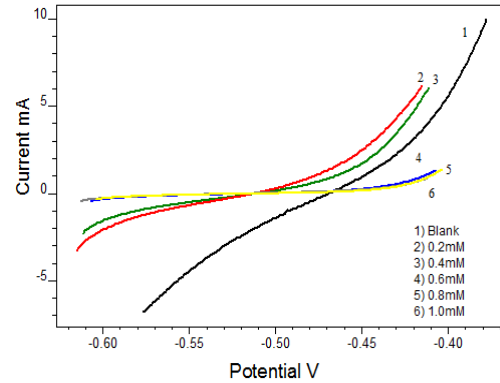


Fig. 3.37b Linear polarization curves of MS in the presence and absence of CTHMT2YBA in 1.0M HCl

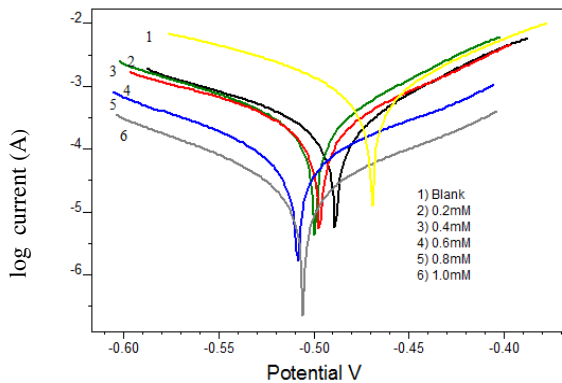


Fig. 3.38a Tafel plots of MS in the presence and absence of CTHMF2YBA in 1.0M HCl

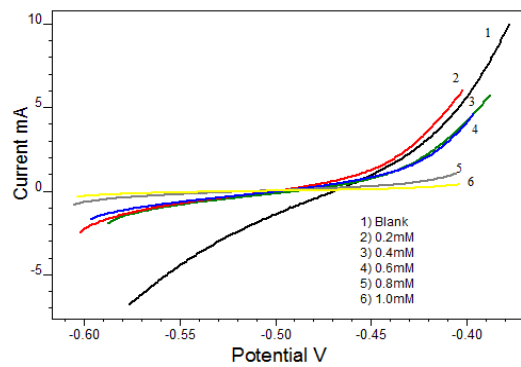


Fig. 3.38b Linear polarization curves of MS in the presence and absence of CTHMF2YBA in 1.0M HCl

On analyzing the data presented in Table 3.7, it can be found that the anodic and cathodic slope variations are different for each inhibitor. I3YT2YMAPA was found to be predominantly cathodic type. For the inhibitors T2YMABA, CTHMT2YBA and CTHMF2YBA the cathodic slope is slightly varied suggesting that these molecules are acting on both the cathode and anode and thus can be regarded as a mixed type inhibitor. Whereas PHMT2YBA molecules acted as anodic inhibitor. Generally if the shift of E_{corr} is greater than 85 with respect to E_{corr} of uninhibited solution along with the considerable change of anodic or cathodic slopes, the inhibitor can be viewed as cathodic or anodic

type. Figure 3.39 represents a comparison of corrosion inhibition efficiencies of all Schiff base inhibitors. According to polarization studies, the general trend of inhibition efficiency follows the order I3YT2YMAPA > PHMT2YBA > CTHMT2YBA > T2YMABA > CTHMF2YBA. This order is same as that obtained from weight loss method.

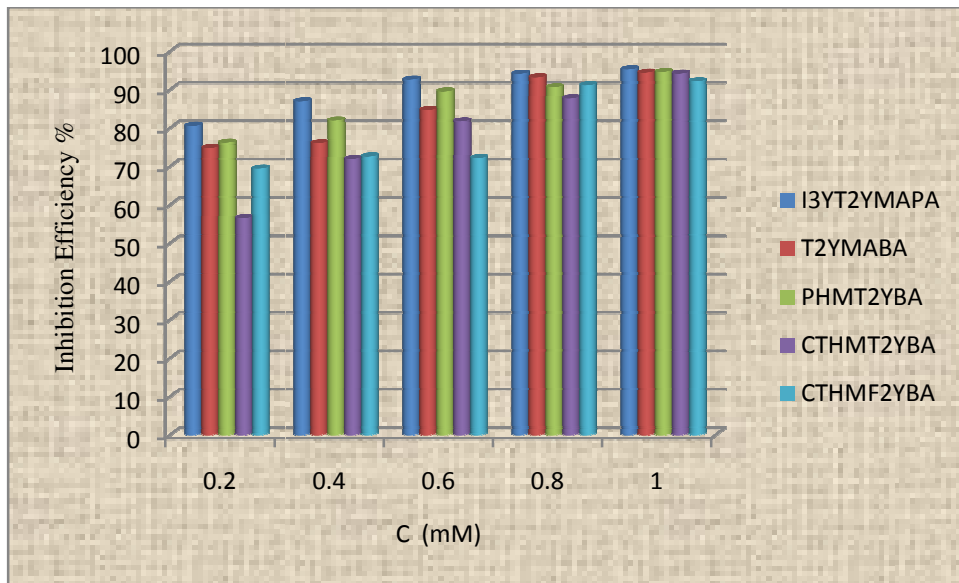


Fig. 3.39 Comparison of corrosion inhibition efficiencies ($\eta_{\text{pol}}\%$) of Schiff bases I3YT2YMAPA, T2YMABA, PHMT2YBA, CTHMT2YBA and CTHMF2YBA on MS in 1.0M HCl

Mechanism of inhibition

It is well known that the surface of the metal is positively charged in acidic media. It is believed that the Cl^- ions can be specifically adsorbed on the metal surface and creates an excess of negative charge on the surface⁷². This will favour the adsorption of protonated inhibitor on the surface and hence reduce the dissolution of Fe to Fe^{2+} . Besides this electrostatic interaction between the protonated inhibitor and the metal surface, other possible interactions are i) interaction of unshared electron pairs in the molecule with the metal ii) interaction of π -electrons with the metal and iii) a

combination of types (i–ii). If one examines the structures of Schiff bases, many potential sources of inhibitor–metal interaction can be recognized. The unshared pair of electrons present on N atoms in each inhibitor is of key importance in making coordinate bond with the metal. The π -electron cloud of the aromatic rings and the azomethine linkage also participate in the inhibition mechanism. Furthermore, the double bonds in the inhibitor molecule permit the back donation of metal d electrons to the π^* orbital and this type of interaction cannot occur with amines⁷³. This can be justified by the lower inhibition efficiency of the parent amines than that of Schiff base inhibitors. Figure 3.40 illustrate the mechanism of action of inhibitor molecules on the metal surfaces.

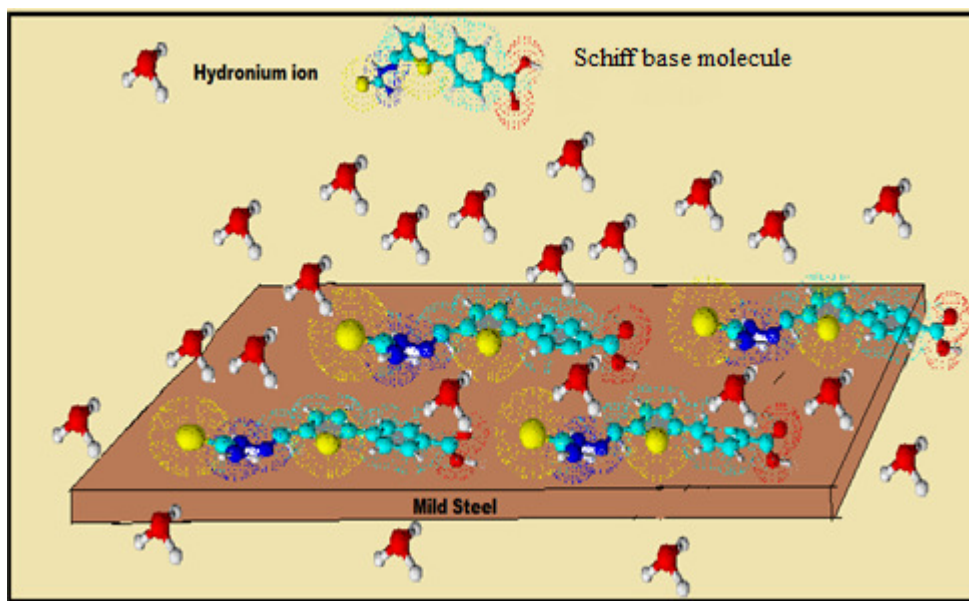


Fig. 3.40 Mechanism of corrosion inhibition by Schiff base inhibitor molecules on MS surface

SECTION II

CORROSION INHIBITION STUDIES OF SCHIFF BASE INHIBITORS I3YT2YMAPA, T2YMABA, PHMT2YBA, CTHMT2YBA AND CTHMF2YBA ON MILD STEEL IN 0.5M H₂SO₄

The corrosion inhibition of the mild steel specimens are studied in 0.5M sulphuric acid solution. Different methods like weight loss measurements, electrochemical impedance studies and potentiodynamic polarisation studies were performed and are detailed in this section. Generally it was found that the inhibition efficiencies of the Schiff base inhibitors in 0.5M H₂SO₄ medium were not that much pronounced as in the hydrochloric acid medium. Sulphuric acid being more aggressive than hydrochloric acid will cause a higher rate of corrosion of mild steel specimens.

Weight loss studies

The mild steel specimens were immersed in 0.5M sulphuric acid medium for 24 hours in the presence and absence of inhibitors. Corrosion rates and inhibition efficiency values characteristic of each compound are given in Tables 3.8 and 3.9.

The Schiff base inhibitor I3YT2YMAPA exhibited least corrosion rates compared to other compounds. The inhibition performance of this compound was the highest ie, 92% at a concentration of 1.0mM. Generally as the inhibitor concentration is increased the inhibition efficiency also increased for all the inhibitors. The aromatic rings in addition to the azomethane linkage and highly polarizable S atom make the molecule to attract the surface metal atoms strongly which results in the greater inhibition performance.

Table 3.8 Corrosion rates ($\text{mm} \cdot \text{y}^{-1}$) of MS in the presence of Schiff base inhibitors I3YT2YMAPA, T2YMABA, PHMT2YBA, CTHMT2YBA and CTHMF2YBA in 0.5M H_2SO_4

C(mM)	I3YT2YMAPA	T2YMABA	PHMT2YBA	CTHMT2YBA	CTHMF2YBA
0	26.11	26.11	26.11	26.11	26.11
0.2	16.76	24.97	24.83	24.68	15.99
0.4	12.21	22.09	22.98	21.38	15.88
0.6	10.01	20.67	18.67	19.14	10.78
0.8	7.36	16.05	17.09	14.93	10.35
1.0	5.98	14.13	12.33	12.65	9.05

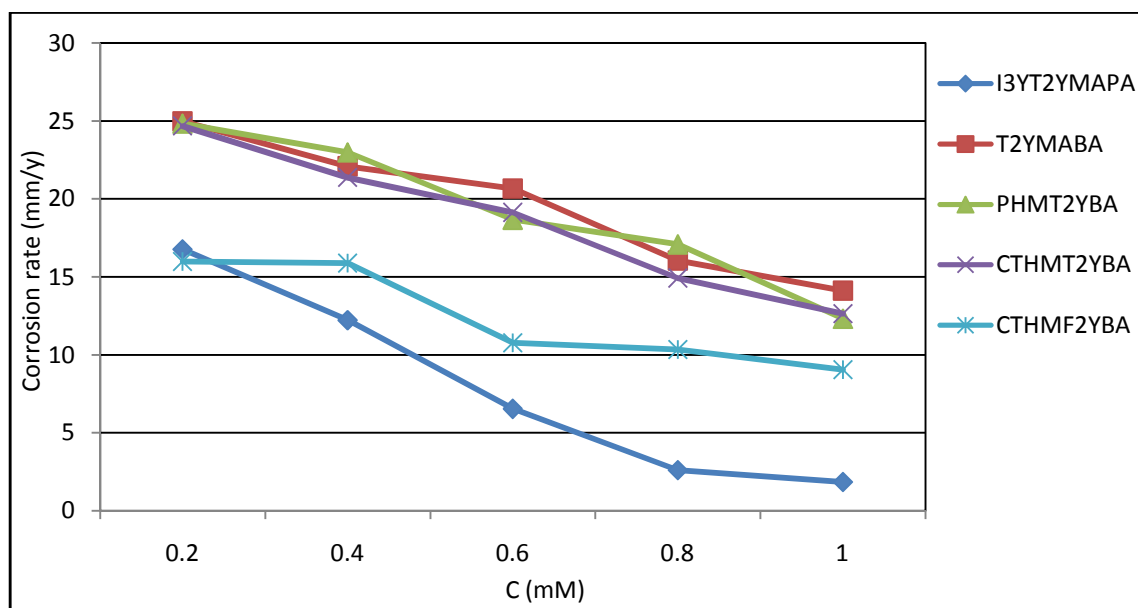


Fig. 3.41 Variation of corrosion rates of MS with the concentration of Schiff base inhibitors I3YT2YMAPA, T2YMABA, PHMT2YBA, CTHMT2YBA and CTHMF2YBA in 0.5M H_2SO_4

Schiff base inhibitors T2YMABA, PHMT2YBA and CTHMT2YBA showed comparatively poor corrosion inhibition efficiency on MS surface in 0.5M H_2SO_4 medium. Eventhough these molecules possesses active corrosion inhibition probes, they displayed lower corrosion inhibition power, which may be attributed to a) high corrosive nature of

sulphuric acid medium and b) intensive hydrolysis of these inhibitors in sulphuric acid medium. The furfural derived Schiff base inhibitor CTHMF2YBA showed fair corrosion inhibition efficiency on MS surface. Comparison of corrosion rates and inhibition efficiencies are demonstrated in Figures 3.41 and 3.42 respectively.

Table 3.9 Inhibition efficiencies of Schiff base inhibitors I3YT2YMAPA, T2YMABA, PHMT2YBA, CTHMT2YBA and CTHMF2YBA on MS in 0.5M H₂SO₄

C (mM)	Inhibitors				
	I3YT2YMAPA	T2YMABA	PHMT2YBA	CTHMT2YBA	CTHMF2YBA
0.2	35.81	4.35	4.88	1.18	38.75
0.4	53.21	15.39	11.96	5.46	39.15
0.6	61.69	20.84	28.50	18.09	58.72
0.8	71.81	38.53	34.55	26.67	60.36
1.0	77.09	45.89	52.79	51.56	65.32

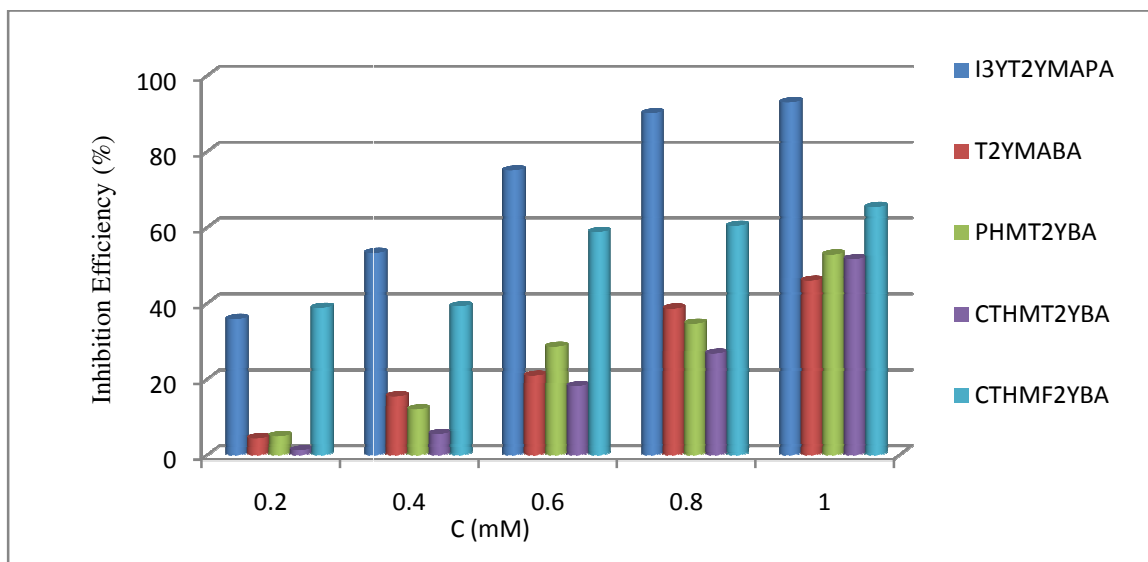


Fig. 3.42 Comparison of corrosion inhibition efficiencies ($\eta_w\%$) of Schiff base inhibitors I3YT2YMAPA, T2YMABA, PHMT2YBA, CTHMT2YBA and CTHMF2YBA on MS in 0.5M H₂SO₄

Adsorption isotherms

The adsorption isotherms help to verify the mechanism of interaction of the inhibitor on the surface of MS specimens. Different adsorption isotherms were considered and the best fit model of isotherm was selected with the aid of correlation coefficient. The adsorption isotherms are represented in Figures 3.43-3.47.

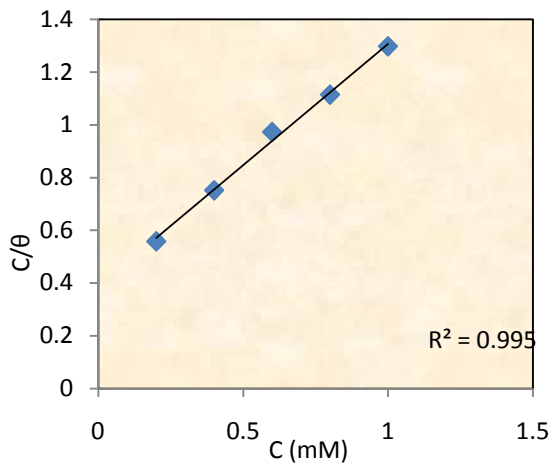


Fig. 3.43 Langmuir adsorption isotherm for I3YT2YMAPA on MS in 0.5M H₂SO₄

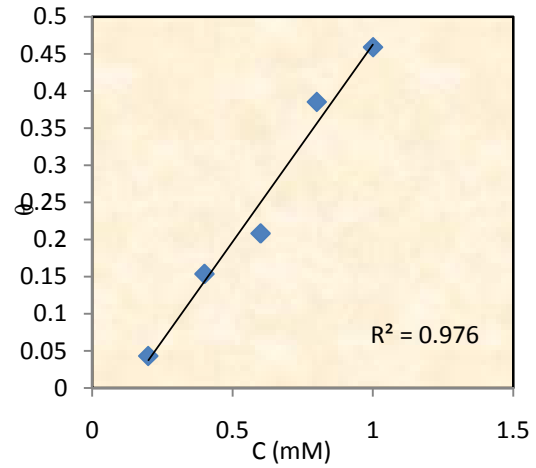


Fig.3.44 Freundlich adsorption isotherm for T2YMABA on MS in 0.5 M H₂SO₄

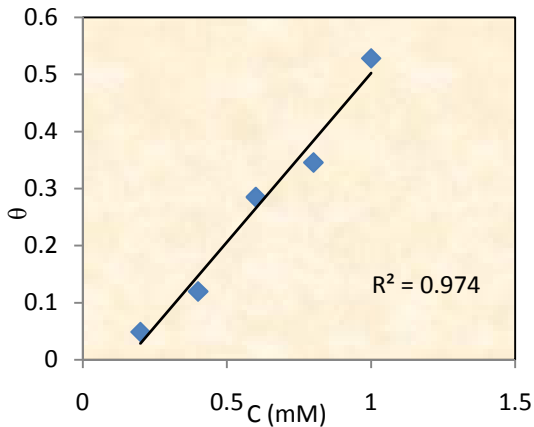


Fig. 3.45 Freundlich adsorption isotherm for PHMT2YBA on MS in 0.5M H₂SO₄

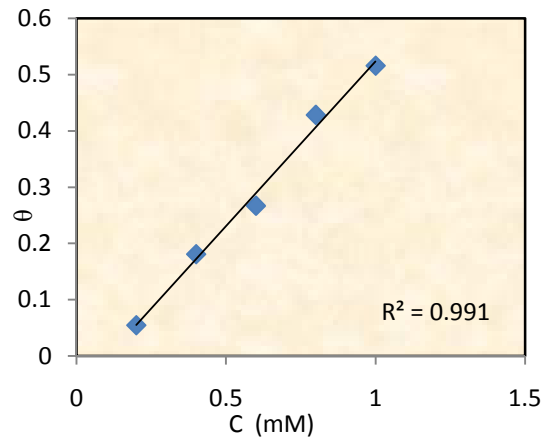


Fig. 3.46 Freundlich adsorption isotherm for CTHMT2YBA on MS in 0.5 M H₂SO₄

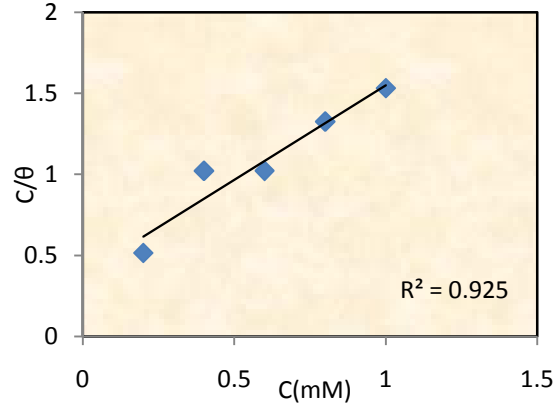


Fig. 3.47 Langmuir adsorption isotherm for CTHMF2YBA on MS in 0.5M H₂SO₄

The best fit adsorption isotherm for T2YMABA, PHMT2YBA and CTHMT2YBA was Freundlich isotherm, which can be represented as

$$\theta = K_{ads} C$$

where C is the concentration of the inhibitor, θ is the fractional surface coverage and K_{ads} is the adsorption equilibrium constant. At the same time for I3YT2YMAPA and CTHMF2YBA inhibitors, Langmuir isotherm was the suitable one. Langmuir adsorption isotherm can be represented as

$$\frac{C}{\theta} = \frac{1}{K_{ads}} + C$$

K_{ads} and ΔG_{ads}^0 , are calculated for each inhibitor and are reported in Table 3.10. The negative value of free energy of adsorption indicates the spontaneity of the process. In the present investigation ΔG_{ads}^0 values for all the molecules suggested that the adsorption involved both physisorption and chemisorption. The low values of the adsorption equilibrium constant for T2YMABA, PHMT2YBA and CTHMT2YBA were an indication of possibility of multilayer adsorption of these molecules on the metal surface. Inhibitors I3YT2YMAPA and CTHMF2YBA exhibited high values of K_{ads} and ΔG_{ads}^0 suggesting that there was a monolayer of protective molecules formed on the surface

through chemical interaction. Even though the rates of corrosion of metal specimens were high in sulphuric acid, it can be concluded that these molecules were able to make an effective protection barrier preventing the dissolution of Fe atoms.

Table 3.10 Thermodynamic parameters for the adsorption of Schiff base inhibitors I3YT2YMAPA, T2YMABA, PHMT2YBA, CTHMT2YBA and CTHMF2YBA on MS in 0.5M H₂SO₄

Parameter	I3YT2YMAPA	T2YMABA	PHMT2YBA	CTHMT2YBA	CTHMF2YBA
Isotherm	Langmuir	Freundlich	Freundlich	Freundlich	Langmuir
K _{ads}	2590	531	592	609	2611
ΔG _{ads} (kJ/mol)	-30	-25.75	-26.03	-26.1	-30

Surface morphological studies

The effect of I3YT2YMAPA molecules on MS surface was studied with SEM analyses. SEM images of MS surfaces in the absence of medium, in the presence of corroding medium (0.5M H₂SO₄) and in the presence of corroding medium and inhibitor are given in Figures 3.48-3.50 respectively. On comparing Figures 3.48 and 3.49, it can be established that the surface of MS was seriously damaged in the acidic solution. Figure 3.50 represents the surface image of the metal in the presence of the I3YT2YMAPA molecules (0.1mM, 24 h). Morphology of this image clearly proved that the damage occurred for the surface was fairly reduced in presence of the inhibitor.

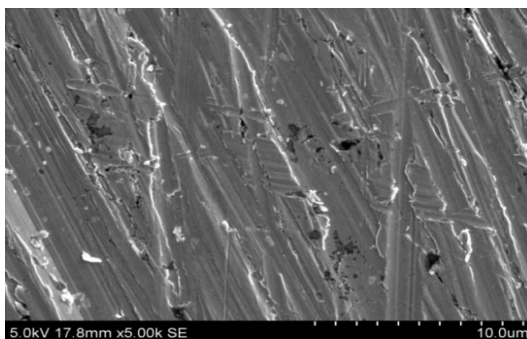


Fig. 3.48 SEM image of the bare MS

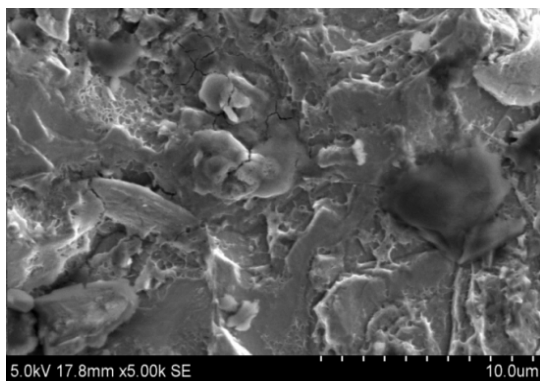


Fig. 3.49 SEM image of MS surface in 0.5M H₂SO₄ after 24 h

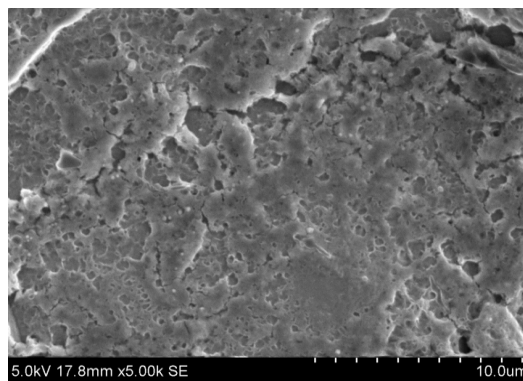


Fig. 3.50 SEM image of MS surface in 0.5M H₂SO₄ and I3YT2YMAPA after 24 h

Corrosion inhibition studies on parent compounds

Corrosion inhibition characteristics of the parent compounds of each Schiff base inhibitor were studied and compared. The results are given in table 3.11.

The parent compounds consists of 2-amino-3-(3-indolyl)propanoic acid (AIPA), 3-amino benzoic acid (ABA), thiocarbamoylhydrazide (TCH), phenyl hydrazine (PH), 4-(5-formylthiophen-2-yl)benzoic acid (FT2YBA) and 4-(5-formylfuran-2-yl)benzoic acid (FF2YBA). These compounds were taken in 0.2, 0.6 and 1.0mM concentrations in 0.5M H₂SO₄ and their inhibition efficiencies against MS corrosion for a period of 24 hours were studied using gravimetric method.

Table 3.11 Corrosion inhibition efficiencies ($\eta_w\%$) of parent compounds AIPA, 3ABA, FT2YBA, FF2YBA, TCH and PH on MS surface in 0.5M H₂SO₄

C (mM)	AIPA	3ABA	FT2YBA	FF2YBA	TCH	PH
0.2	4.27	4.14	30.75	49.21	1.89	20.85
0.6	28.31	10.83	41.34	57.65	8.14	32.64
1.0	52.24	21.35	53.64	62.32	18.5	40.01

On comparison, it can be inferred that the higher inhibition performance of the Schiff base inhibitor were due to the presence of azomethine linkage in them. The amino acid, 2-amino-3-(3-indolyl)propanoic acid (AIPA) gave a highest 52% inhibition at 1.0mM concentration whereas the Schiff base inhibitor produced a much better result at the corresponding concentration i.e.; 77%. The parent amine ABA and TCH showed very little activity in sulphuric acid medium. The arylated compounds of thiophene-2-carboxaldehyde and furan-2-carboxaldehyde gave somewhat better efficiencies. The presence of aromatic rings in them might have improved their inhibition character.

Electrochemical studies on corrosion

Electrochemical methods involve impedance and potentiodynamic measurements in sulphuric acid medium. Electrochemical impedance measurements are quick when compared to the weight loss measurements.

The five novel Schiff base inhibitors were subjected to electrochemical corrosion inhibition studies on MS in 0.5M H₂SO₄ medium. EIS and Tafel polarization studies were performed to get a quick and reliable result on the inhibition capacities of the inhibitors on mild steel.

Electrochemical impedance spectroscopic (EIS) studies

The EIS experiments were carried out on an Ivium compact stat-e electrochemical system. 1M HCl was taken as the electrolyte and the working area of the metal specimens were exposed to the electrolyte for 1 h prior to the measurement. EIS measurements were performed at constant potential (OCP) in the frequency range from 1 KHz to 100 mHz with amplitude of 10 mV as excitation signal. The mild steel specimens were subjected to EIS measurements in sulphuric acid medium in the absence and presence of the inhibitors. Different concentrations of the Schiff base inhibitors were prepared and the

working electrode of the EIS system was made into contact with these solutions. Impedance plots, Nyquist plots (or Cole-Cole plot) and Bode plots were obtained in acid medium. The plots are given in Figures 3.51-3.55. The impedance parameters like charge transfer resistance (R_{ct}), solution resistance (R_s), double layer capacitance (C_{dl}) and percentage inhibition efficiency ($\eta_{EIS}\%$) calculated from the R_{ct} values are given in the Table 3.12. The percentage of inhibitions of each Schiff base were calculated using charge transfer resistance values by the following expression

$$\eta_{EIS} \% = \frac{R_{ct} - R'_{ct}}{R_{ct}} \times 100$$

where R_{ct} and R'_{ct} are the charge transfer resistances of working electrode with and without inhibitor respectively.

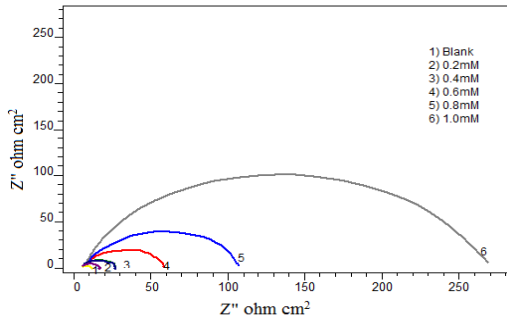


Fig. 3.51a Nyquist plots of MS in the presence and absence of I3YT2YMAPA in 0.5M H_2SO_4

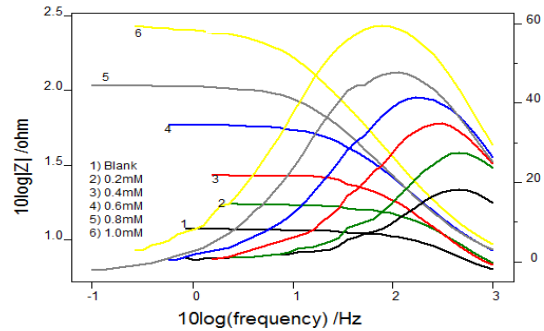


Fig. 3.51b Bode plots of MS in the presence and absence of I3YT2YMAPA in 0.5M H_2SO_4

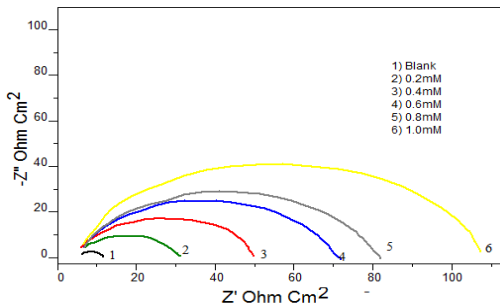


Fig. 3.52a Nyquist plots of MS in the presence and absence of T2YMABA in 0.5M H_2SO_4

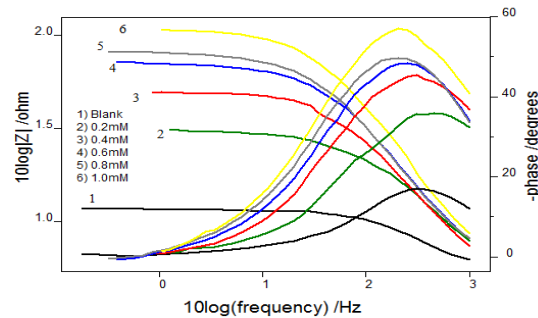


Fig. 3.52b Bode plots of MS in the presence and absence of T2YMABA in 0.5M H_2SO_4

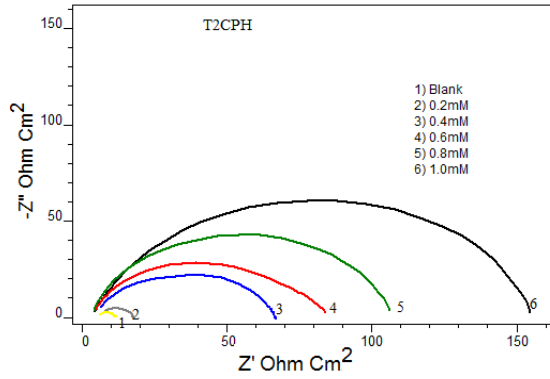


Fig. 3.53a Nyquist plots of MS in the presence and absence of PHMT2YBA in 0.5M H₂SO₄

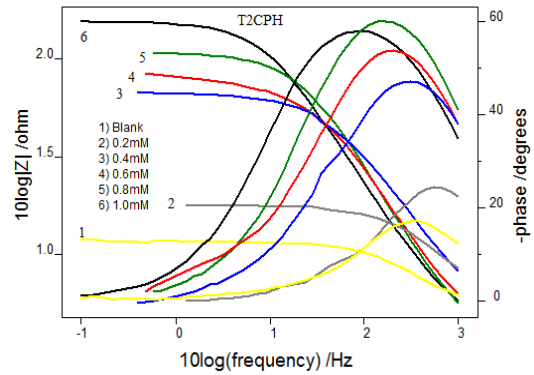


Fig. 3.53b Bode plots of MS in the presence and absence of PHMT2YBA in 0.5M H₂SO₄

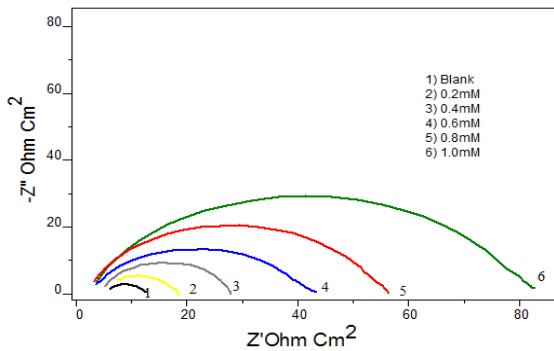


Fig. 3.54a Nyquist plots of MS in the presence and absence of CTHMT2YBA in 0.5M H₂SO₄

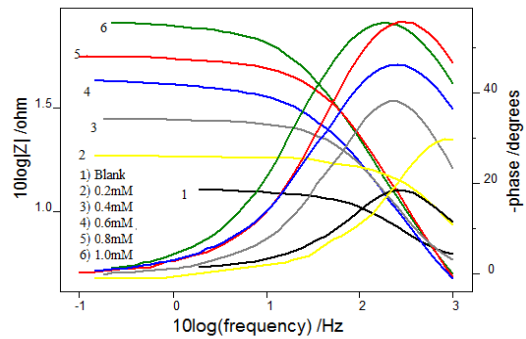


Fig. 3.54b Bode plots of MS in the presence and absence of CTHMT2YBA in 0.5M H₂SO₄

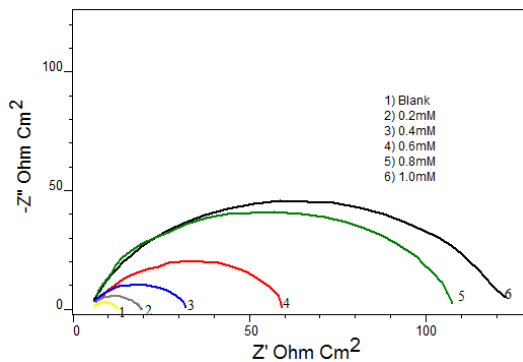


Fig. 3.55a Nyquist plots of MS in the presence and absence of CTHMF2YBA in 0.5M H₂SO₄

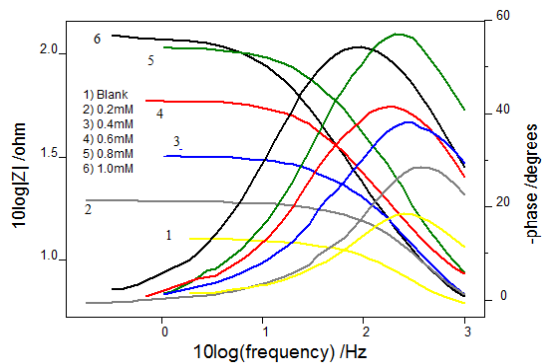


Fig. 3.55b Bode plots of MS in the presence and absence of CTHMF2YBA in 0.5M H₂SO₄

It is evident from the plots that the impedance response of metal specimens showed a marked difference in the presence and absence of the inhibitors. The Schiff base I3YT2YMAPA showed the highest R_{ct} value 232. R_{ct} is a measure of electron transfer across the exposed area of the metal surface and it is inversely proportional to rate of corrosion. This compound showed the highest inhibition efficiency of 97% at 1.0mM concentration. Inhibitors T2YMABA, PHMT2YBA, CTHMT2YBA and CTHMF2YBA also exhibited appreciable inhibition capacities against corrosion. PHMT2YBA showed significant inhibition efficiency (80%) even at the lowest concentration taken of 0.2mM. Generally the R_{ct} values were found to increase with increasing inhibitor concentration. Decrease in capacitance values CPE with inhibitor concentration can be attributed to the decrease in local dielectric constant and /or increase in the thickness of the electrical double layer. This emphasizes the action of inhibitor molecules by adsorption at the metal–solution interface. The percentage of inhibition ($\eta_{EIS} \%$) showed a regular increase with increase in inhibitor concentration for all the Schiff base inhibitors and this trend is represented in Figure 3.56.

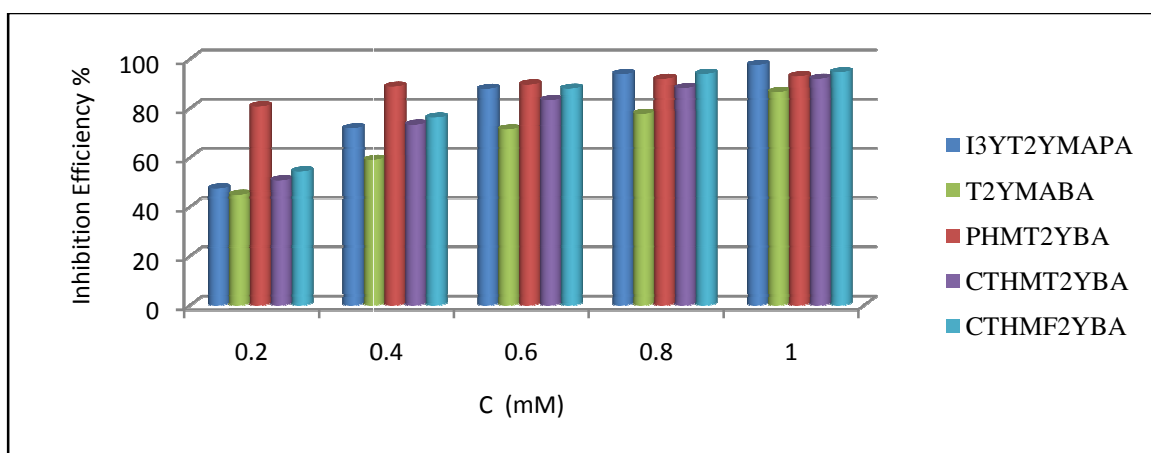


Fig.3.56 Comparison of corrosion inhibition efficiencies ($\eta_{EIS}\%$) of Schiff base inhibitors I3YT2YMAPA, T2YMABA, PHMT2YBA, CTHMT2YBA and CTHMF2YBA on MS in 0.5M H_2SO_4

Table 3.12 Electrochemical impedance parameters of MS in the presence and absence of Schiff base inhibitors I3YT2YMAPA, T2YMABA, PHMT2YBA, CTHMT2YBA and CTHMF2YBA in 0.5 M H₂SO₄

Inhibitor	C (mM)	C _{dl}	R _{ct}	η _{EIS} %
	0	116	5.57	-
I3YT2YMAPA	0.2	89.8	10.6	47.45
	0.4	84.5	19.8	71.86
	0.6	77.2	46	87.89
	0.8	69.1	90	93.81
	1.0	70.1	232	97.59
	T2YMABA	0.2	129	10.1
0.4		107	13.6	59.04
0.6		167	19.5	71.43
0.8		123	25	77.72
1.0		95	41.5	86.57
PHMT2YBA	0.2	79	28.9	80.73
	0.4	113	49.6	88.77
	0.6	63.7	53.8	89.64
	0.8	75.6	68.9	91.91
	1.0	69.6	79.6	93.00
CTHMT2YBA	0.2	42.9	11.3	50.71
	0.4	10.2	20.9	73.34
	0.6	12.3	33.3	83.27
	0.8	9.8	47.1	88.17
	1.0	7.7	69.2	91.95
CTHMF2YBA	0.2	82.7	12.2	54.34
	0.4	80.5	23.4	76.19
	0.6	76.6	46.3	87.96
	0.8	46.3	92.5	93.97
	1.0	10.2	104	94.64

The inhibition efficiencies resulted from EIS analysis are higher than that obtained from gravimetric studies and these results are not comparable. Since electrochemical analysis is a rapid corrosion monitoring technique it will only exhibit the corrosion inhibition capacities of molecules on MS at the early stage of treatment. The molecules will gradually hydrolyze into their parent compounds and thus show poor inhibition efficiency in H₂SO₄ medium for a long span of 24 hours. That's why gravimetric corrosion inhibition results are lower than the electrochemical results. Comparatively least efficiency was reported in the case of inhibitor T2YMABA. Even at the highest concentration (1mM) it has showed 86.57% inhibition efficiency. The order of performances of the studied Schiff base inhibitors on MS can be given as I3YT2YMAPA > CTHMF2YBA > PHMT2YBA > CTHMT2YBA > T2YMABA.

Potentiodynamic polarization studies

The behaviors of the present inhibitors towards polarization of metal specimens were studied by Tafel extrapolation analysis and linear polarization studies. Polarization studies were performed by recording anodic and cathodic polarization curves. Polarization plots were obtained in the electrode potential range from -100 to +100 mV Vs corrosion potential (E_{corr}) at a scan rate of 1mV/sec. Tafel polarization analysis were done by extrapolating anodic and cathodic curves to the potential axis to obtain corrosion current densities(I_{corr}). The percentage of inhibition efficiency (η_{pol}%) was evaluated from the measured I_{corr} values using the following relation

$$\eta_{\text{pol}} \% = \frac{I_{\text{corr}} - I'_{\text{corr}}}{I_{\text{corr}}} \times 100$$

where I_{corr} and I' _{corr} are the corrosion current densities of the exposed area of the working electrode in the absence and presence of inhibitor respectively. From the polarization

analyses, polarization parameters like corrosion current densities (I_{corr}), corrosion potential (E_{corr}), cathodic Tafel slope (b_c) and anodic Tafel slope (b_a) were determined and are listed in Table 3.13. Using these parameters percentage of inhibition efficiency ($\eta_{\text{pol}}\%$) for MS specimens was determined. From the slope analysis of the linear polarization curves at the vicinity of corrosion potential of blank as well as at different concentrations of the inhibitor, the values of polarization resistance (R_p) in acid solution were obtained. From the evaluated polarization resistance, the inhibition efficiency was calculated using the relationship

$$\eta_{R_p} \% = \frac{R'_p - R_p}{R'_p} \times 100$$

where R'_p and R_p are the polarization resistance in the presence and absence of the inhibitor respectively.

It is evident, from the Tafel parameters for the inhibition of various Schiff base inhibitors on metal surface, that the corrosion current density (I_{corr}) was decreased with increasing the inhibitor concentration. From linear polarization analysis it can be seen that the polarization resistance was considerably increased with the inhibitor concentration for all the studied inhibitors. This behavior can be attributed to the increase of adsorption of the molecules with concentration. The I3YT2YMAPA molecules showed a highest of 97.59% inhibition efficiency at 1.0mM concentration in the Tafel analysis. This was followed by compound CTHMF2YBA, which has got 94.85% efficiency at the highest concentration. Other Schiff bases also gave good inhibition performances; all of them showing >30 % inhibition capacity even at the lowest concentration (0.2mM). The Tafel curves and linear polarization curves are given in Figures 3.57-3.61.

Table 3.13 Potentiodynamic polarization parameters in the presence and absence of Schiff base inhibitors I3YT2YMAPA, T2YMABA, PHMT2YBA, CTHMT2YBA and CTHMF2YBA in 0.5M H₂SO₄

Inhibitor	Tafel data					Linear polarization data		
	C (mM)	-E _{corr} (mV/SCE)	I _{corr} (μA/cm ²)	-b _c (mV/dec)	b _a (mv/dec)	η _{pol} %	R _p (ohm)	η _{Rp} %
	0	472	1443	131	91	-	12.5	-
I3YT2YMAPA	0.2	471	733	112	66	49.20	21.08	40.70
	0.4	472	656	115	75	54.54	25.7	51.36
	0.6	418	359	117	69	75.12	46.48	73.11
	0.8	496	110	122	102	92.38	156.5	92.01
	1.0	463	34.7	86	36	97.59	274.3	95.44
T2YMABA	0.2	483	899	86	164	37.69	19	34.21
	0.4	460	571	62	108	60.43	30.18	58.58
	0.6	481	401	66	141	72.21	38.1	67.19
	0.8	482	367	72	123	74.57	42.56	70.63
	1.0	478	232	58	130	83.92	60.46	79.34
PHMT2YBA	0.2	520	850	112	90	41.09	48	73.96
	0.4	478	199	104	63	86.21	60	79.17
	0.6	501	359	117	69	75.12	86.5	85.55
	0.8	481	80.1	92	45	84.45	113.5	88.98
	1.0	498	122	90	84	91.55	115	89.13
CTHMT2YBA	0.2	527	484	100	80	66.46	32	60.94
	0.4	458	451	103	63	68.75	34	63.24
	0.6	473	320	107	69	77.82	48	73.95
	0.8	493	205	98	68	85.79	69	81.88
	1.0	478	158	103	71	89.05	94	86.70
CTHMF2YBA	0.2	-520	951	125	106	34.09	26.2	52.29
	0.4	478	231	130	58	83.99	75.2	83.38
	0.6	501	172	100	74	88.08	106.9	88.31
	0.8	481	141	97	79	90.23	133.5	90.64
	1.0	498	132	96	84	94.85	147	91.49

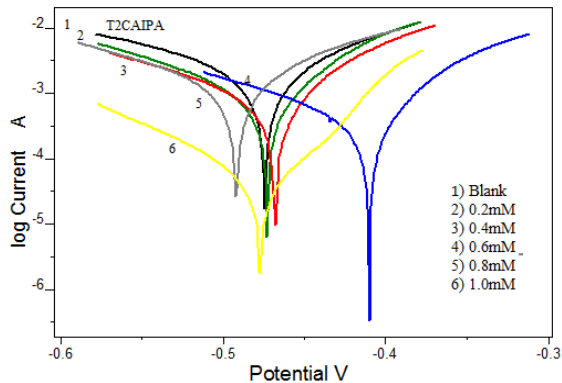


Fig. 3.57a Tafel plots of MS in the presence and absence of I3YT2YMAPA in 0.5M H₂SO₄

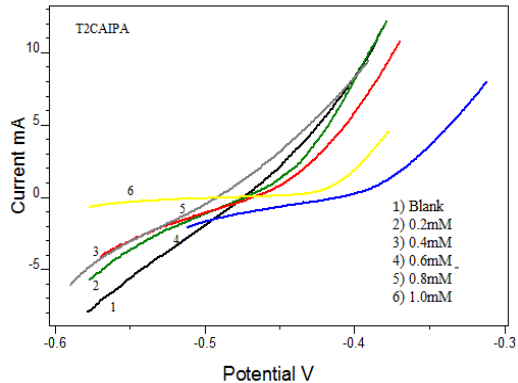


Fig. 3.57b Linear polarization curves of MS in the presence and absence of I3YT2YMAPA in 0.5M H₂SO₄

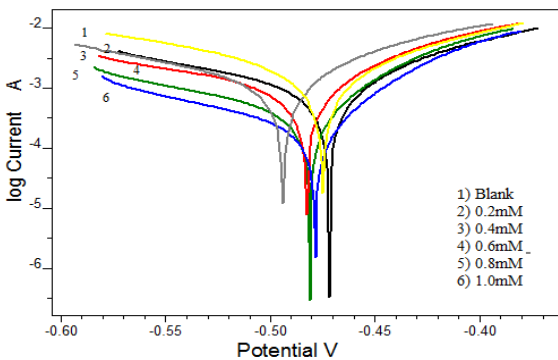


Fig. 3.58a Tafel plots of MS in the presence and absence of T2YMABA in 0.5M H₂SO₄

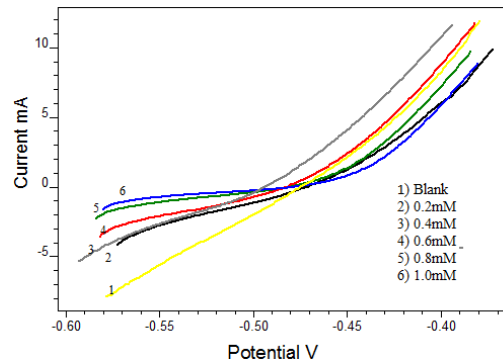


Fig. 3.58b Linear polarization curves of MS in the presence and absence of T2YMABA in 0.5M H₂SO₄

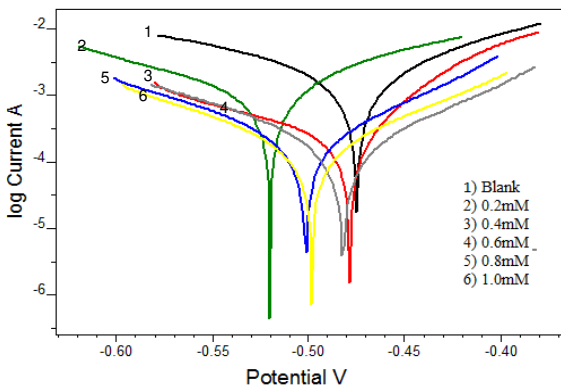


Fig. 3.59a Tafel plots of MS in the presence and absence of PHMT2YBA in 0.5M H₂SO₄

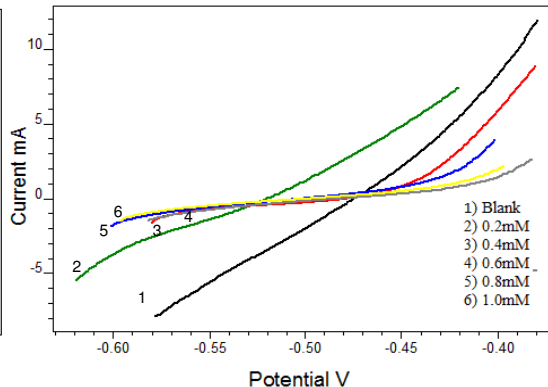


Fig. 3.59b Linear polarization curves of MS in the presence and absence of PHMT2YBA in 0.5M H₂SO₄

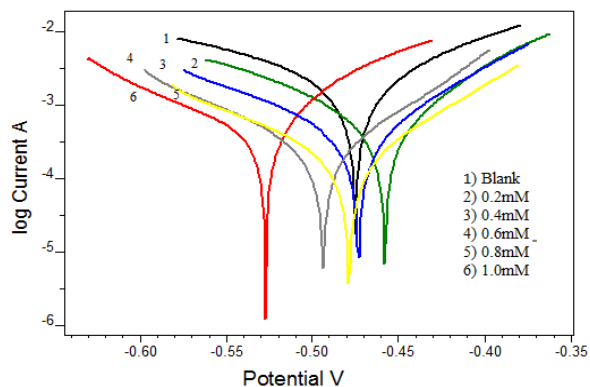


Fig. 3.60a Tafel plots of MS in the presence and absence of CTHMT2YBA in 0.5M H_2SO_4

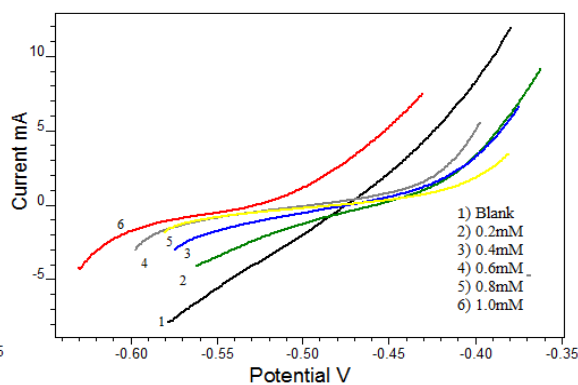


Fig. 3.60b Linear polarization curves of MS in the presence and absence of CTHMT2YBA in 0.5M H_2SO_4

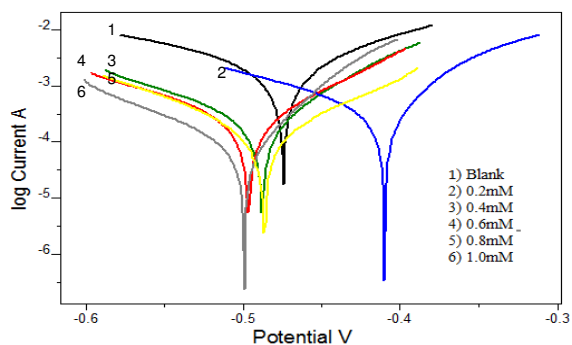


Fig. 3.61a Tafel plots of MS in the presence and absence of CTHMF2YBA in 0.5M H_2SO_4

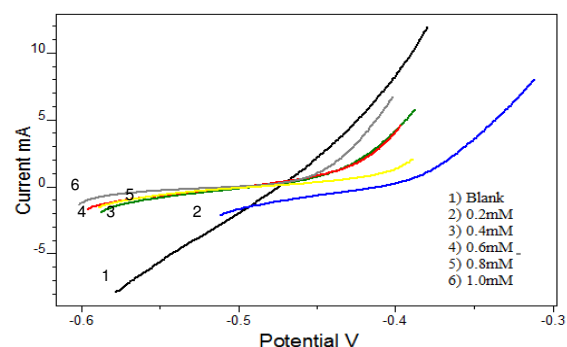


Fig. 3.61b Linear polarization curves of MS in the presence and absence of CTHMF2YBA in 0.5M H_2SO_4

Even though the inhibitors T2YMABA, PHMT2YBA and CTHMT2YBA showed very poor inhibitive capacity at 24h as per weight loss studies, their corrosion inhibition power according to the polarization studies were much higher than that expected. The presence of hetero atoms, aromatic rings and azomethine linkage present in the molecule would result in the enhanced the corrosion inhibition of these inhibitors. On close examination of the Tafel slopes, it is evident that these compounds namely I3YT2YMAPA, T2YMABA and PHMT2YBA showed much variations in cathodic and anodic slopes which suggest that they could affect the anodic and cathodic sites of corrosion and hence be called as mixed corrosion inhibitors. In the case of

CTHMT2YBA, the cathodic slope variation was not that much pronounced, compared with others and therefore this molecule can be regarded as a anodic inhibitor. Corrosion potential (E_{corr}) of MS specimens did not change appreciably during all the measurements. The corrosion inhibition efficiencies of Schiff base inhibitors are in the order I3YT2YMAPA > CTHMF2YBA > PHMT2YBA > CTHMT2YBA > T2YMABA which is same as the result of EIS measurements. A comparison of inhibition efficiencies are given in Figure 3.62.

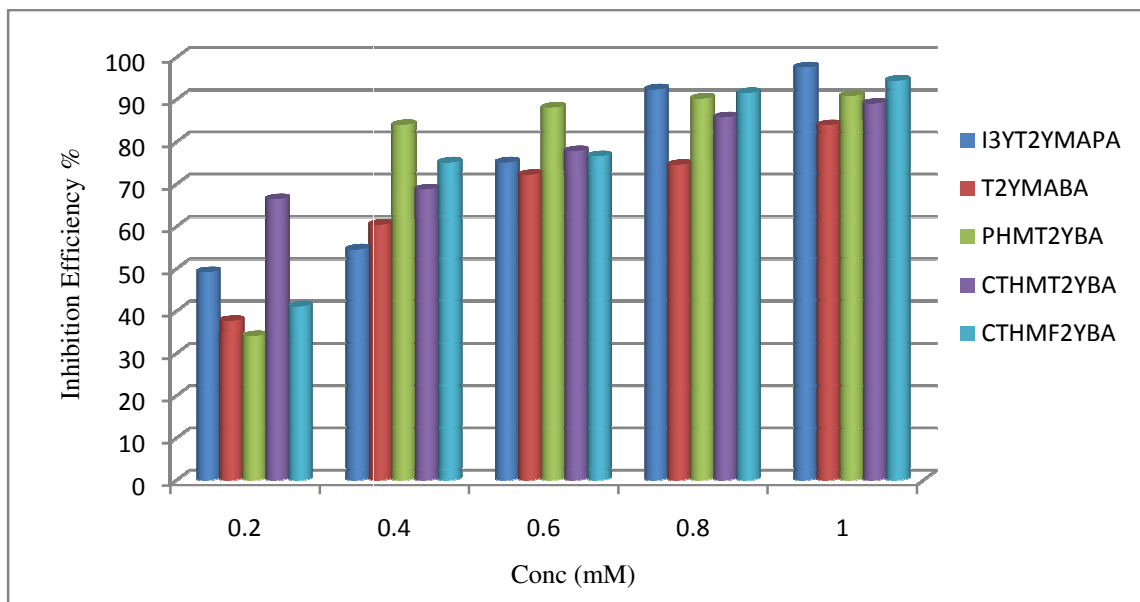


Fig. 3.62 Comparison of corrosion inhibition efficiencies ($\eta_{\text{pol}}\%$) of Schiff base inhibitors I3YT2YMAPA, T2YMABA, PHMT2YBA, CTHMT2YBA and CTHMF2YBA on MS in 0.5M H_2SO_4

SUMMARY

The corrosion inhibition efficiencies of newly synthesized heterocyclic Schiff base inhibitors namely 3-(1H-indol-3-yl)-2-[(E)-(thiophen-2-ylmethylidene)amino]propanoic acid (I3YT2YMAPA), (E)-3-(thiophen-2-ylmethylene amino)benzoic acid (T2YMABA), (E)-4-(5-((2-carbamothioylhydrazono)methyl)thiophen-2-yl)benzoic acid (CTHMT2YBA), (E)-4-(5-((2-phenylhydrazono)methyl)thiophen-2-yl)benzoic acid (PHMT2YBA) and (E)-4-(5-((2-carbamothioylhydrazono)methyl)furan-2-yl)benzoic acid (CTHMF2YBA) against MS specimens in 1.0M HCl and 0.5M H₂SO₄ solutions were analysed using weight loss studies and electrochemical methods such as electrochemical impedance spectroscopy (EIS) and potentiodynamic polarization studies. It was found that all the inhibitors exhibited very good corrosion inhibition property on mild steel in HCl medium. Generally the corrosion inhibition efficiency was poor in H₂SO₄ medium than in HCl medium. Adsorption studies and surface morphological analysis were conducted to establish the mechanism of corrosion inhibition of these inhibitors.

According to the weight loss studies in HCl medium, the inhibition efficiencies were increased with the inhibitor concentrations for all the compounds. At a maximum concentration of 1.0mM, all the studied inhibitors displayed 70-83% inhibition efficiencies by the weight loss studies. At the electrochemical studies, they performed very potential anticorrosive activity (92-96%) towards MS at 1.0mM concentration. The compound I3YT2YMAPA exhibited the highest inhibition performance against mild steel (96.16%). The electron density of the aromatic ring systems, azomethine linkage and highly polarisable sulphur atom are the root causes by which the molecule showed better inhibition efficiency. Adsorption studies revealed that Freundlich isotherm was the

best fit isotherm for I3YT2YMAPA, PHMT2YBA, CTHMT2YBA and CTHMF2YBA molecules whereas Langmuir isotherm was followed by T2YMABA in 1.0M HCl medium. The values of thermodynamic parameters suggested that adsorption process was spontaneous and the interaction between the metal and inhibitor molecules involves both electrostatic-adsorption and chemisorptions. The role of azomethine group in the inhibitory action was proved when the parent compounds of the Schiff base inhibitors were taken for corrosion studies. The activities were higher for the Schiff bases than the parent compounds. The corrosion inhibition performances of the compounds at elevated temperatures were also studied in HCl medium. Data obviously established that the rate of corrosion is increased at elevated temperatures.

The electrochemical studies on corrosion in HCl medium were performed and the order of inhibition capacity of bases was the same as that obtained from gravimetric studies, I3YT2YMAPA > PHMT2YBA > CTHMT2YBA > T2YMABA > CTHMF2YBA. Potentiodynamic polarization studies suggested that all inhibitors acted as a mixed type inhibitors for MS specimens in 1.0M HCl. Generally it is noticed that the inhibition efficiencies of these Schiff base inhibitors are quite higher by electrochemical studies than weight loss studies.

In 0.5M sulphuric acid medium, the gravimetric studies gave a different order of corrosion inhibition efficiency for the Schiff base inhibitors, i.e. I3YT2YMAPA > CTHMF2YBA > PHMT2YBA > CTHMT2YBA > T2YMABA. A maximum of 77.1% was obtained by I3YT2YMAPA at 1mM concentration. The inhibition efficiencies were lesser than that in HCl medium, which can be explained with the aggressive nature of the sulphuric acid. Weight loss measurements on both Schiff base inhibitors and their

corresponding parent compounds were performed and compared. Langmuir isotherm was the best fit one for I3YT2YMAPA and CTHMF2YBA and Freundlich isotherm for others. The ΔG_{ads}^0 values for all the molecules suggested that the adsorption involved both physisorption and chemisorption.

Electrochemical impedance and potentiodynamic investigations in 0.5M H₂SO₄ gave higher corrosion inhibition efficiencies compared to gravimetric studies. Inhibition efficiency greater than 95% was expressed by I3YT2YMAPA in both experiments. I3YT2YMAPA, T2YMABA and PHMT2YBA showed much variations in cathodic and anodic slopes which suggest that these molecules could affect the anodic and cathodic sites of corrosion and can be called as mixed corrosion inhibitors. In the case of CTHMT2YBA, the cathodic slope variation was not that much pronounced when compared with others, and hence this molecule was regarded as an anodic inhibitor.

REFERENCES

- 1) S. R. Rao, “*Resource Recovery And Recycling From Metallurgical Wastes*”, Elsevier, (2006) 179.
- 2) L. David, Liptak, G. Bela, “*Environmental Engineers' Handbook*”, CRC Press, (1997) 973.
- 3) C.G. Munger, “*Corrosion Prevention By Protective Coatings*”, NACE (1999).
- 4) M. Behpour, S. M. Ghoreish, A. Gandomi, N. Niasar, N. Soltani, M. Niasari M, *J. Mater. Sci.*, 44 (2009) 2444.
- 5) H. Shorky, M. Yuasa, I Sekine , R.M. Issa, H.Y. El-Baradie, G.K. Gomma, *Corros. Sci.*, 40 (1998) 2173.
- 6) S. Sankarap, F. Apavinasam, M. Pushpanaden, F. Ahmed, *Corros. Sci.*, 32 (1991) 193.
- 7) K. Yesim, G. Seda, E. Asli, *Prot. Met. Phys. Chem. Surf.*, 48 (2012) 710.
- 8) A. Asan, S. Soylu, T. Kiyak, F. Yıldırım, S. G. Oztas, N. Ancın, M. Kabasakaloglu, *Corros. Sci.*, 48 (2006) 3933.
- 9) E. Sputnik, Z. Ademovic, *Proceedings of the 8th European Symposium on Corrosion Inhibitors*, (1995) 257.
- 10) B.G. Clubby, *Chemical Inhibitors for Corrosion Control*, Royal Soc. Chem., Cambridge, (1990) 141.
- 11) M. Gojic, L. Kosec, *ISIJ Int.*, 37 (7) (1997) 685.
- 12) M. Metikos Hukovic, R. Babic, Z. Grubac, S. Brinic, *J. Appl. Electrochem.*, 24 (1994) 325.
- 13) L. Kobotiatis, N. Pebere, P.G. Koutsookos, *Corros. Sci.*, 41 (1999) 41.

- 14) V. Guillaumin, G. Mankowski, *Corros. Sci.*, 41 (1999) 421.
- 15) W. Quafsaoui, C.H. Blanc, N. Beberé, A. Srhiri, G. Mankowski, *J. Appl. Electrochem.*, 30 (2000) 959.
- 16) C. Blanc, S. Gastaud, G. Mankowski, *J. Electrochem. Soc.*, 150 (2003) 396.
- 17) A. Mozalev, A. Poznyok, I. Mazaleva, A.W. Hassel, *Electrochem. Com.*, 3 (2001) 299.
- 18) E. E. Ebenso, P. C. Okafor, U. J. Eppe, *Anticorr. Meth. Mat.*, 50 (6) (2003) 414.
- 19) I. N. Putilova, S. A. Balizin, V. P. Baranmik, *Metallic Corrosion Inhibitors*, Pergaman Press, London, (1960).
- 20) A. Raman, P. Labine, *Reviews on Corrosion Inhibitor Science and Technology*, NACE, Houston, TX, 1 (1986) 20.
- 21) M. Hosseini, S.F.L. Mertens, M. Ghorbani, M.R. Arshadi, *Mater. Chem. Phys.*, 78 (2003) 800.
- 22) A. K. Singh, M. A. Quraishi, *Corros. Sci.*, 52 (2010) 152.
- 23) A. K. Singh, M. A. Quraishi, E. E. Ebenso, *Int. J. Electrochem. Sci.*, 6 (2011) 5673.
- 24) B. Joseph, S. John, A. Joseph, B. Narayana, *Indian J. Chem. Technol.*, 17 (2010) 366.
- 25) P.C. Okafor, Y. Zheng, *Corros. Sci.*, 51 (2009) 850.
- 26) A.M. Shams El Din, A.A. El Hosary, R.M. Saleh, J.M. Abd El-Kader, *Werkst. Corrosion*, 28 (1977).
- 27) M.S. Abdel Aal, A.A. Abdel Wahab, A. El. Saied, *Corrosion (NACE)*, 37 (1981) 557.
- 28) M.N. Desai, P.O. Chauhan, N.K. Shah, *7th Symposium on Corrosion Inhibitors, Ferrara, Italy (1990); 8th Symposium on Corrosion Inhibitors, Ferrara, Italy (1995)*.
- 29) L. Wang, J.X. Pu, H.C. Luo, *Corros. Sci.*, 45 (2003) 677.

- 30) A. K. Singh, M. A. Quraishi, *Int. J. Electrochem. Sci.*, 7 (2012) 3222.
- 31) M. T. Muniandy et. al., *Surf. Rev. Lett.*, 18 (2011)127.
- 32) M.D. Shah, A.S. Patel, G.V. Mudaliar, N.K. Shah, *Portugaliae Electrochim. Acta*, 29(2) (2011) 101.
- 33) S. P. Fakrudeen, H.C. Ananda Murthy, B. Raju, *J. Chilean Chem. Soc.*, 57, 4 (2012) 1364.
- 34) S. Thirugnanaselvi, S. Kuttirani, A. Roseline Emelda, *Science Direct*, 24 (6) (2014) 1969.
- 35) V. Panchal , A. Patel, N. Shah, *Scientific paper*, UDC :620.197.3 :669.715,
- 36) F. B. Ravar, A. Dadgarinezhad, *Gazi University J. Sci.*, 25(4) (2012) 835.
- 37) A. Sorkhabia, B. Shaabanib, D. Seifzadeha, *Appl. Surf. Sci.*, 239 (2005) 154.
- 38) T. Sethi, A. Chaturvedi, R.K. Upadhyay, S. P. Mathur, *J. Chilean Chem. Soc.*, 52, 3 (2007) 1206.
- 39) R. K. Upadhyay, S. P. Mathur, *E-Journal of Chemistry.net*. 4(3) (2007) 408.
- 40) M. Yadav, D. Behera, S. Kumar, *Canadian Metallurgical Quarterly*, 53(2) (2014) 220.
- 41) A. A. Al-Amiery, A. A. H. Kadhum, A. Hameed M. A., Abu Bakar Mohamad,H. Pua Soh, *Materials*, 7 (2014) 662.
- 42) Jeyaprabha, S. Muralidharan, D. Jayaperumal, G. Venkatachari, N.S. Rengaswamy *Antcorr. Meth. Mat.*, 45(3) (1998) 148.
- 43) X. Li, S. Deng, H. Fu, T. Li, *Electrochim. Acta*, 54 (2009) 4089.
- 44) E. Kamis, *Corrosion*, 46 (1990) 478.

- 45) S. S. Abd El-Rehim, A. Magdy, M. Ibrahim, F. Khaled, *J. Appl. Electrochem.*, 29 (1999) 599.
- 46) E. McCafferty, H. Leidheiser Jr., “*Corrosion Control By Coating*”, Science Press, Princeton, (1979).
- 47) E. Cano, J.L. Polo, A. La Iglesia, J.M. Bastidas, *Adsorption*, 3 (2004) 219.
- 48) M. Bouklah, N. Benchat, B. Hammouti, A. Aouniti, S. Kertit, *Mater. Lett.*, 60 (2006) 1901.
- 49) J. O’M. Bockris, A. K. N. Reddy, “*Modern Electrochemistry-2*”, Plenum Press, New York, (1970).
- 50) E. Gileadi, “*Electrode Kinetics For Chemists, Chemical Engineers And Material Scientists*”, VCH publishers, New York (1993).
- 51) D. A. Jones, “*Principles and Prevention of Corrosion*”, Macmillam publishing, New York, (1992).
- 52) R. Baboian, “*Electrochemical Techniques for Corrosion*”, National association of corrosion engineers, Houston, TX (1977).
- 53) U. Bertocci, F. Mansfeld, “*Electrochemical Corrosion Testing*”, ASTM STP 727, ASTM international, West Conshohocken, PA (1979).
- 54) H. H. Uhlig, R. W. Revie, “*Corrosion And Corrosion Control*”, John Wiley & Sons, New York, (1985).
- 55) E. Barsoukov, J. R. Macdonald, “*Impedance Spectroscopy, Theory, Experiment and Applications*”, Wiley Interscience publications, New York, 2nd Ed., (2005).
- 56) F. Mansfield, *Electrochim. Acta*, 35 (1990) 1533.
- 57) M. Kendig, J. Scully, *J. Electrochem. Soc.*, 141 (1994) 1823

- 58) F. Mansfeld, M. Kendig, “*Evaluation of Protective Coatings with Impedance measurements*”, International Congress on Metallic corrosion, 3 (1984) 74.
- 59) G. Reinhard, U. Rammelt. *Corrosion*, 15 (1984) 175.
- 60) T. Strivens, C. Taylor, *Mater. Chem.*, 7 (1982) 199.
- 61) F. Mansfeld, M.W. Kendig, *Corrosion*, 37(9) (1981) 545.
- 62) D. D. MacDonald, “*Transient Techniques in Electrochemistry*”, Plenum press. New York, (1977).
- 63) A. Raman, P. Labine “*Reviews on Corrosion Inhibitor Science and Technology*”, NACE, Houston, TX , 1 (1986).
- 64) T. Badea, M. Nicola, I. D. Vaireanu, I. Maior, A. Cojocaru, “*Electrochimie si Corozione, Matrixrom, Bucuresti*”, (2005) 150.
- 65) M. G. Fontana, N. D. Greene, “*Corrosion Engineering*”, McGraw-Hill, New York, (1978).
- 66) M. Stern, A. L. Geary, *J. Electrochem. Soc.*, 105 (1958) 638.
- 67) E. Cano, J. L. Polo, A. La Iglesia, J. M. Bastidas, *Adsorption*, 10(3) (2004) 219.
- 68) P. Bommersbach, C. Alemany-Dumont, J. P. Millet, B. Normand, *Electrochem. Acta*, 51(6) (2005) 1076.
- 69) I. L. Rosenfield, “*Corrosion Inhibitors*”, McGraw-Hill, New York, (1981) 66.
- 70) M. El Azhar, B. Mernari, M. Traisnel, F. Bentiss, M. Lagrenee, *Corros. Sci.*, 43(12) (2001) 2229.
- 71) D. P. Schweinsberg, G.A. George, A. K. Nanayakkara, D. A. Steinert, *Corros. Sci.*, 28(1) (1988) 33.

72) H. Shokry, M. Yuasa, I. Sekine, R. M Issa, H. Y. El-baradie, G. K Gomma, *Corros. Sci.*, 40(12) (1998) 2173.

73) A. K. Singh, M. A. Quraishi, *J. Appl. Electrochem.*, 40(7) (2010) 1293.